ORIGIN OF :

- **GAMMA RAY BURSTS**
  (First Discovered by Vella Satellites, 1967 – Klebsadel et al. 1973)

- **NON SOLAR COSMIC RAYS**
  (Discovered by V. Hess in 1911)

- **HE γ-RAY BACKGROUND RAD**
  (Discovered by Fichtel and Thomson 1982)

- **HE COSMOLOGICAL ν's**
  (To be discovered by xxx, 2004 ?)

Based On Collaboration With
Nicos Antoniou (Athens)
Alvaro De Rújula (CERN)
Rainer Plaga (MPI Munchen)

COSMIC ACCELERATOR | COSMIC BEAM | COSMIC TARGET | γ's ν's

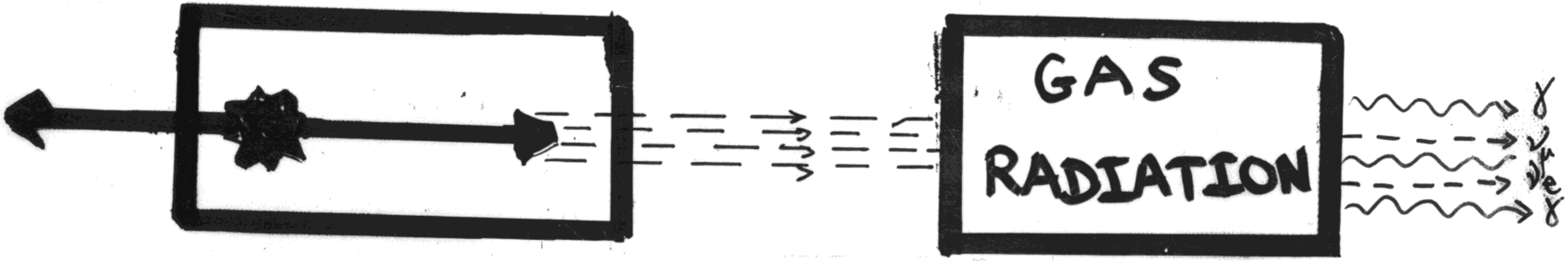

GRB JET | CR | N/cm^2

$$\frac{dn_{\nu_\mu}}{dE} \approx \frac{dn_\gamma}{dE} \sim E^{-2.2}$$

$$\left.\begin{matrix} pp \\ p\gamma \end{matrix}\right\} \rightarrow \left\{\begin{matrix} \pi^\pm \rightarrow \mu\nu_\mu \\ \qquad \mu \rightarrow e\nu_\mu\nu_e \\ \pi^0 \rightarrow 2\gamma \end{matrix}\right.$$

$$F_\nu(E > TeV) \approx 10^{-5\pm1+?}\ erg \cdot cm^{-2} \quad !$$

$$N_{events} \approx 10^{-11\pm1+?}\ cm^{-2}$$

GAMMA RAY BURSTS

$D \sim 10^{28} - 10^{29}$ cm ; $F_\gamma \sim 10^{-4} - 10^{-5} \frac{\text{erg}}{\text{cm}^2}$

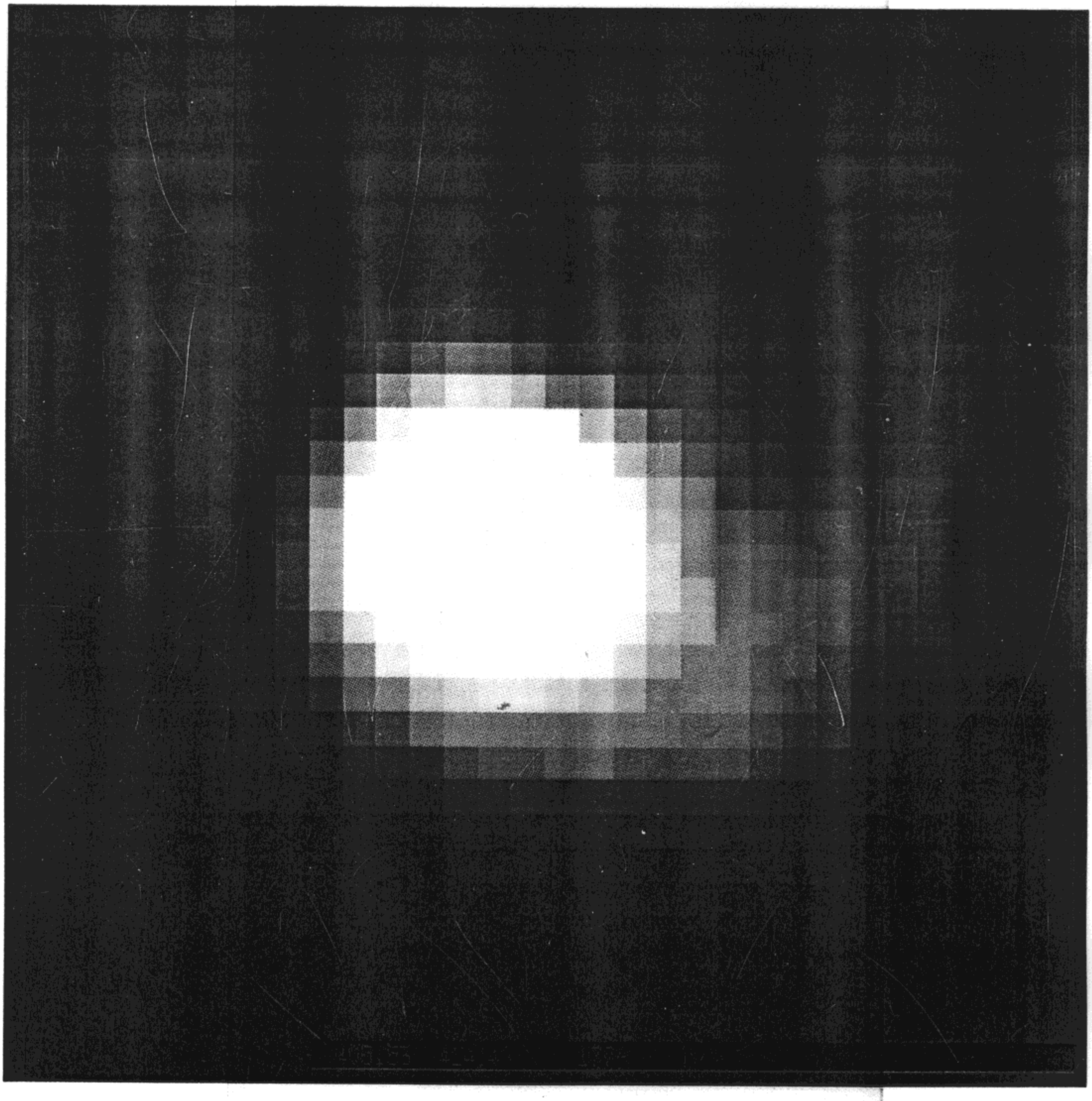

HST observed an extended optical source coincident with the optical transient of GRB 970228

betwen March 26 - April 7 1997

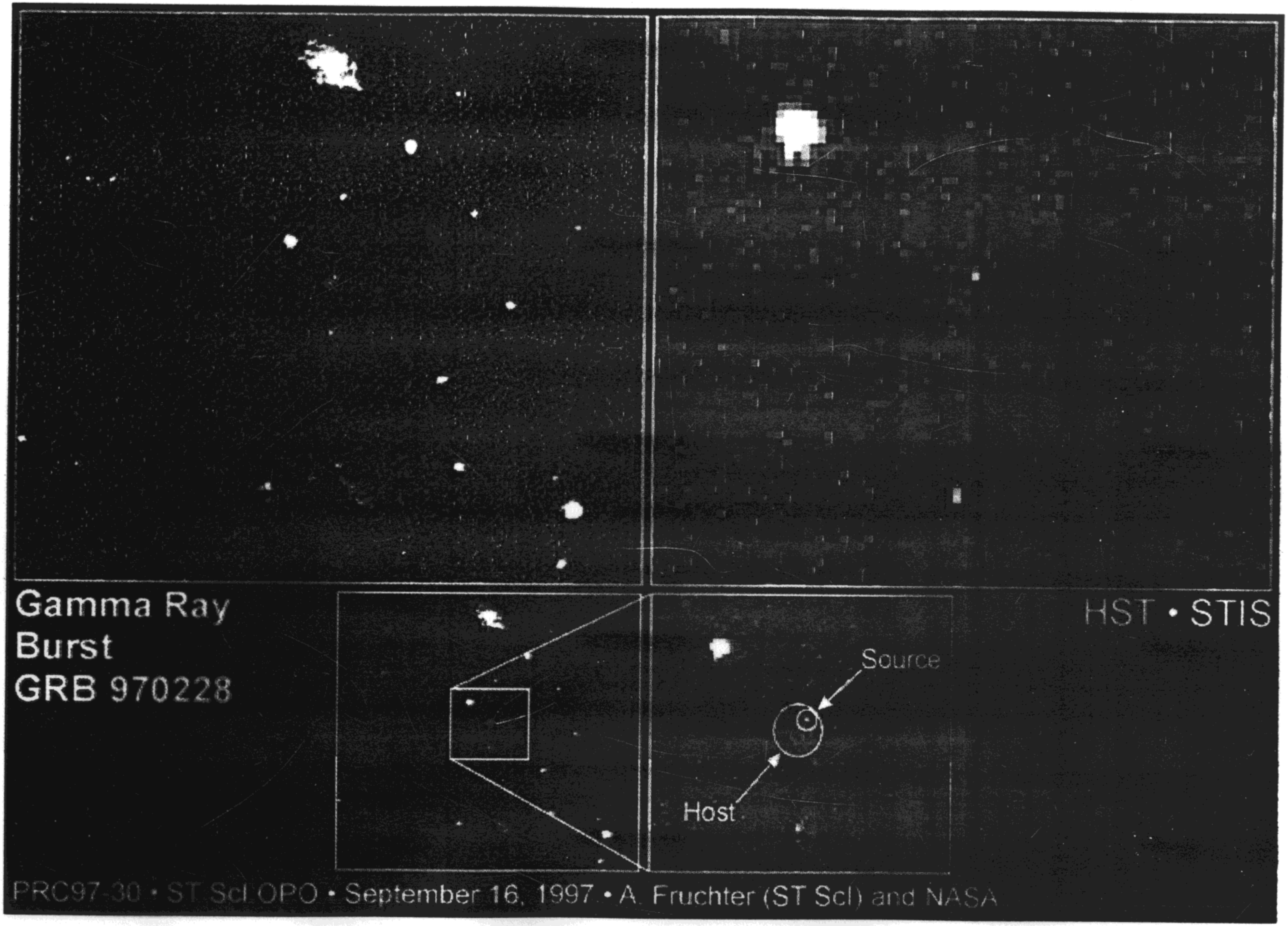

GRB 970228 OT (NASA STScI Press Conference) September 4.65–4.76 UT

GRB 990123

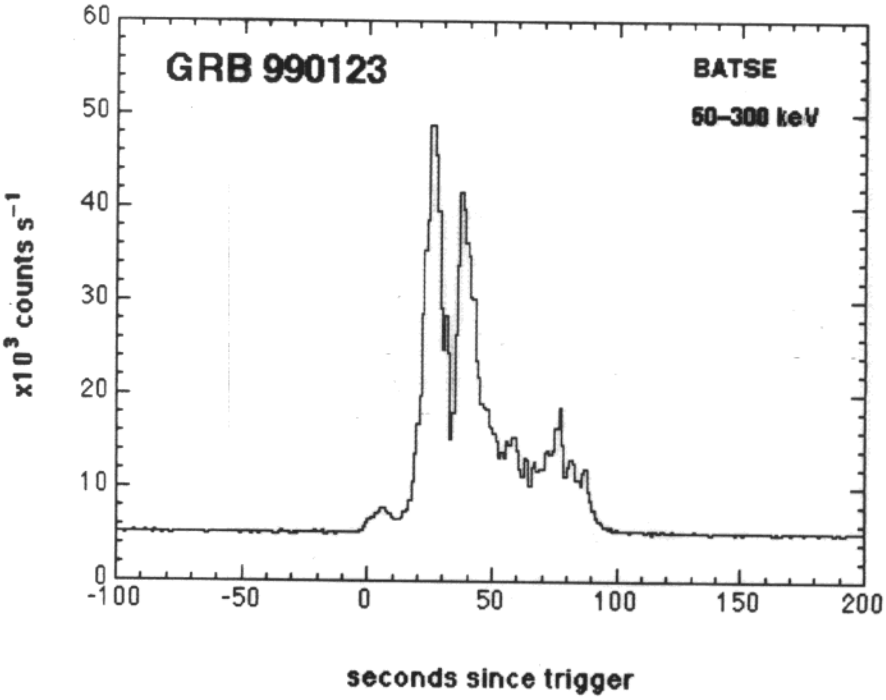

$F_\gamma(50\,\text{keV} < E_\gamma < 300\,\text{keV})$

$5.09 \times 10^{-4} \ \frac{\text{erg}}{\text{cm}^2}$

$z = 1.61$

$\Rightarrow D_L > 3.7 \times 10^{28}\ \text{cm} = 12.0\ \text{Mpc}$

$$\Delta E(50\,\text{keV} < E_\gamma < 300\,\text{keV}) = \frac{4\pi D_L^2 F_\gamma}{1+z} > 3.4 \times 10^{54}\ \text{erg}$$

Largest Explosion Detected After Big-Bang!

Disovery of the Optical Glow of GRB 99012
22.18 seconds after the Nominal BATSE
using the ROTSE-I Telephoto Camera Array/Los

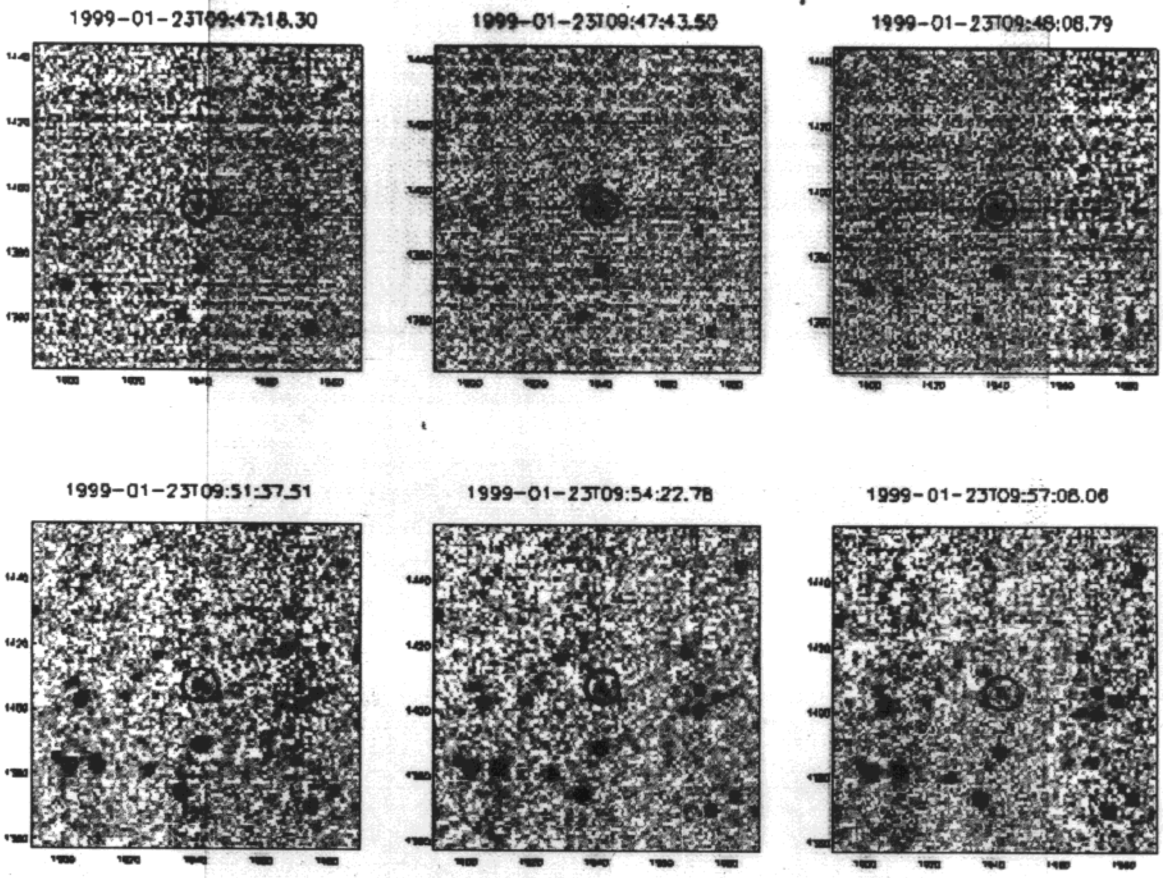

5 s exposu

75 s exposu

TITLE: GCN GRB OBSERVATION REPORT
NUMBER: 205
SUBJECT: GRB990123, early optical counterpart detection
DATE: 99/01/23 23:15:16 GMT
FROM: Carl Akerlof at U.Michigan <akerlof@mich1.physics.lsa.umich.edu>

C. W. Akerlof and T. A. McKay (Univ. of Michigan) report on behalf of the ROTSE collaboration (Michigan/LANL/LLNL):

We observed the error box of GRB 990123 provided by the BACODINE Burst Position Notice dated 23-Jan-99 09:46:59 using the ROTSE-I telephoto camera array located at Los Alamos, New Mexico. The first exposure began at 9:47:18.30, 22.18 seconds after the nominal burst trigger time. A rapidly fading object was discovered at the coordinates, RA = 231.3754, DEC = 44.7666 (J2000) which is within 1/3 of a pixel of the optical counterpart reported by Odewahn et al. (GCN #201). The light curve for this object is relatively complex: the luminosity increases by 3 magnitudes between the first and second exposures. Estimated magnitudes for the first six exposures are given below:

UTC	exposure	m_v
9:47:18.3	5 secs.	11.82
9:47:43.5	5 secs.	8.95
9:48:08.8	5 secs.	10.08
9:51:37.5	75 secs.	13.22
9:54:22.8	75 secs.	14.00
9:57:08.1	75 secs.	14.53

$L = 1.4\times10^{52}\ erg\cdot s^{-1} \approx 3.7\times10^{18} L_\odot$

Note that the ROTSE-I detector system uses an unfiltered broadband CCD so that magnitude estimates are based on comparisons to catalog values for nearby stars. Sky patrol images of the same coordinates taken 133 minutes earlier showed no evidence of the transient to a limit of at least two magnitudes deeper. A more extensive analysis of this data will be available in the near future.

$L_{MW} \approx 2.3\times10^{10} L_\odot$ $\quad \bar{L}_{Quasar} \sim 2.6\times10^{11} L_\odot$

GRB 990123 Energy Crisis

$L_{max} \sim 10^{16} L_G$

$z = 1.61$

$D_L > 3.7 \times 10^{28}$ cm

($h = 0.65$)

BATSE (GCN 224): $5.09 \times 10^{-4} \frac{erg}{cm^2}$

$$E(50 < E_\gamma < 300\,keV) = \frac{4\pi D_L^2 F_\gamma}{1+z}$$

$$E_\gamma > 3.36 \times 10^{54} \frac{\Delta\Omega}{4\pi}\ erg\ !$$

$$\boxed{E \sim 10^{55} \frac{\Delta\Omega}{4\pi}\ erg}$$

Jetted GRB ?

The Afterglow of GRB 990123 Suddenly Declined Fastly. After Feb. 8 Could Not Be Seen By Groun Tels.

HST/STIS Images of GRB 990123

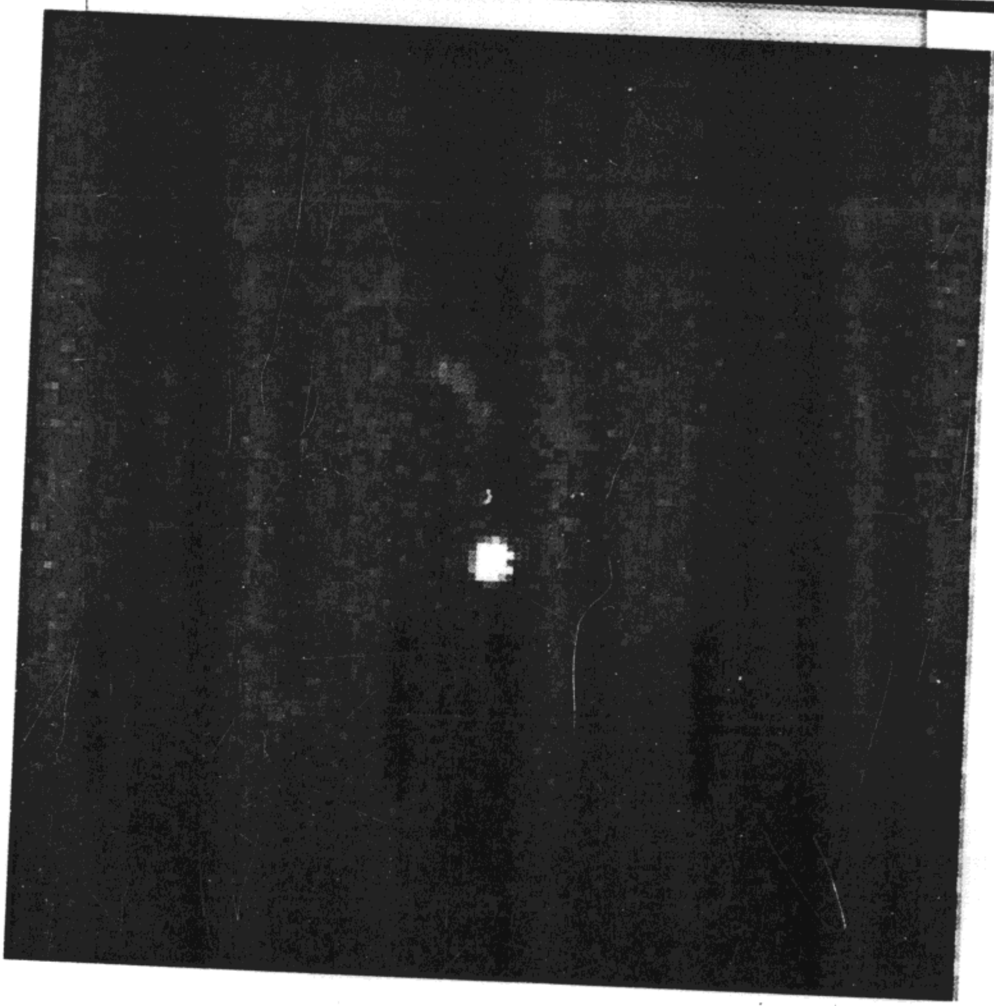

On this page we present the Hubble Space Telescope image of GRB 990123. The Gamma-Ray Burst of January 23, 1999 was first located by the Beppo-Sax satellite, and most remarkably, an optical transient associated with the GRB was detected only ~25 seconds after the start of the burst by a ROTSE camera at Los Alamos. The optical emission peaked about 45 seconds after the start of the burst, at a visual magnitude of about 9. Optical spectra taken at the W.M. Keck Observatory revealed both absorption lines at a redshift of z=1.6. A complete list of notices sent out to the Gamma Ray Burst community on this object Ray Burst community on this object can be found in the GCN Archive.

Here we provide the reduced HST image of GRB 990123 taken Feb 8 1999 23:06 UT and Feb 9 1999 03:21 UT. At the top of this page is a GIF image of the central 3."2 region about the GRB. North is up and East is to the left. The optical transient is seen to be superposed on an irregular galaxy, which could perhaps be an interacting system.

Why Suddenly Fast Decline?

GRB 990123

Fruchter et al. astro-ph/9902236

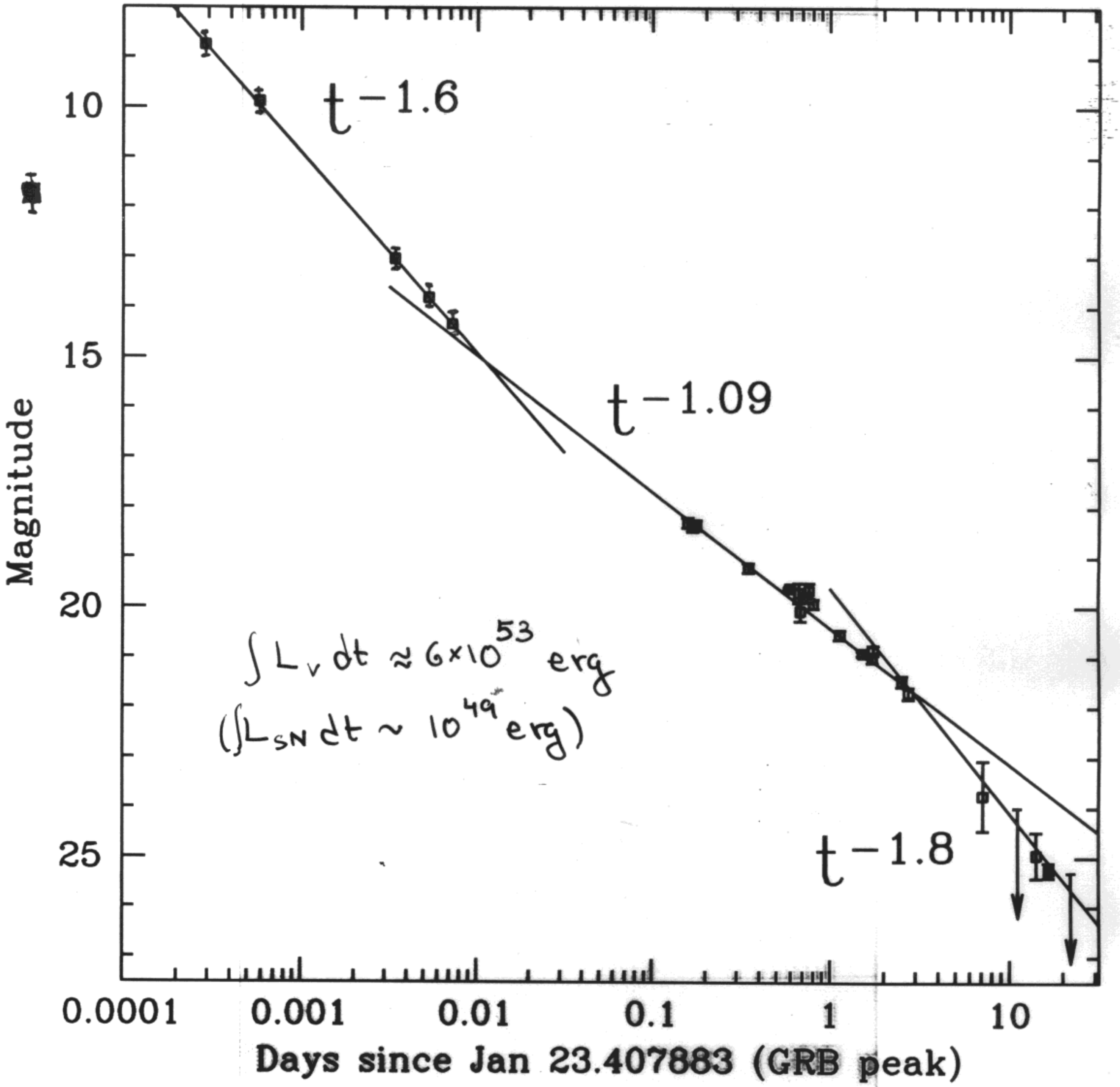

Relativistic Beaming

Rest Frame:

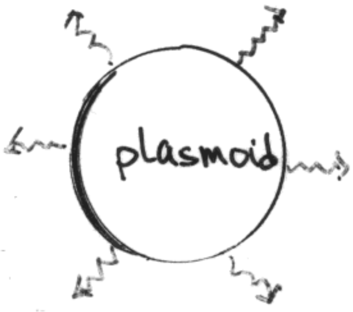

$$I_{\nu'} = h\nu' \frac{dn}{d\nu'} \sim A\nu'^{-\alpha}$$

Lab Frame: $\beta \equiv v/c$; $\Gamma \equiv \dfrac{1}{\sqrt{1-\beta^2}} \gg 1$

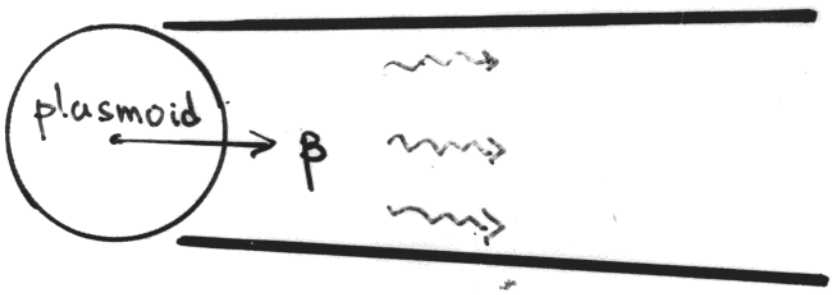

$$\nu = \Gamma(1+\beta\cos\theta')\,\nu'$$

$$\tan\theta = \sin\theta' / \Gamma(\beta+\cos\theta')$$

$$\frac{dI_\nu}{d(\cos\theta)} \approx \frac{4\Gamma^3}{(1+\Gamma^2\theta^2)^3}\, I'\left(\nu' = \nu(1+\theta^2\Gamma^2)/2\Gamma\right)$$

$$\boxed{dI_\nu \approx 4\times 2^{\alpha}\,[\text{redacted}]\,A\nu^{-\alpha} \times \begin{cases} 1; & \Gamma\theta \ll 1/\Gamma \\ (\Gamma\theta)^{-6-2\alpha}; & \Gamma\theta \gg 1 \end{cases}}$$

Amplification

Suppression

Massive Black Hole Accretes Mass (a few $M_\odot$ per year) and Ejects Relativistic Jets That Stop After $\sim 10^6$ Light Years

3C175

10^{60} erg

- Quasar at z=0.768
- Overall linear size 212/*h* kpc (Hubble constant H = 100*h* km/s/Mpc)
- Double lobes with prominent hot spots
- Narrow jet, no counterjet (Doppler hidden?)
- Jet brightens and bends as it enters its lobe
- VLA 4.9 GHz image at 0.35 arcsec resolution

See also Deep VLA Imaging of Twelve Extended 3CR Quasars, by Alan H. Bridle, David H. Hough, Colin J. Lonsdale, Jack O. Burns and Robert A. Laing, *The Astronomical Journal*, **108**, 766-820 (1994). Also related abstract from AAS Meeting #183.

Go back to:

- Alan Bridle's Image Gallery
- Alan Bridle's Home Page
- NRAO Charlottesville Home Page
- NRAO VLA Home Page
- AstroWeb Home Page

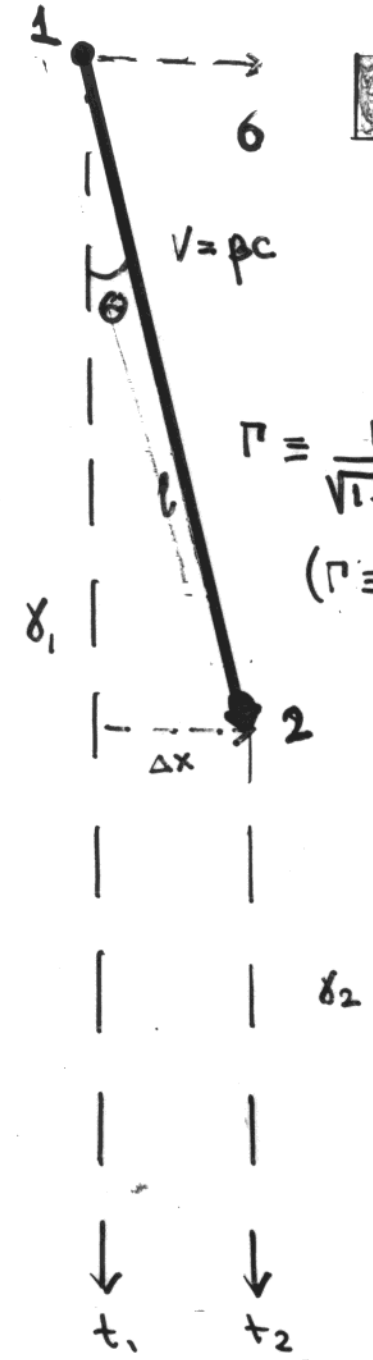

$\boxed{\text{Superluminal Motion}}$

(Rees 1966)

$$\Gamma \equiv \frac{1}{\sqrt{1-\beta^2}} \qquad \left(1-\beta \xrightarrow[\Gamma \gg 1]{} \frac{1}{2\Gamma^2}\right)$$

($\Gamma \equiv$ the Lorentz factor)

arrival times:

$$\Delta x = l \sin\theta$$

$$\Delta t = t_2 - t_1 = \frac{l}{v} - \frac{l\cos\theta}{c} = \frac{l}{c}\left(\frac{1}{\beta} - \cos\theta\right)$$

$$V_\perp \equiv \frac{l\sin\theta}{\frac{l}{c}(1/\beta - \cos\theta)} = \frac{\beta\sin\theta}{1-\beta\cos\theta}\, c$$

$$\Rightarrow \quad V_\perp \approx \frac{2\Gamma^2\theta}{1+\Gamma^2\theta^2}\, c \quad \Rightarrow \quad \boxed{\max V_\perp = \Gamma c}$$

(for $\theta \ll 1$, $\Gamma \gg 1$) $\qquad (\theta_{max} = \frac{1}{\Gamma})$

VLA and VLBI Resolve the Relativistic Jets Into Multiple Ejections of Plasmoid

3C219 = B0917+458

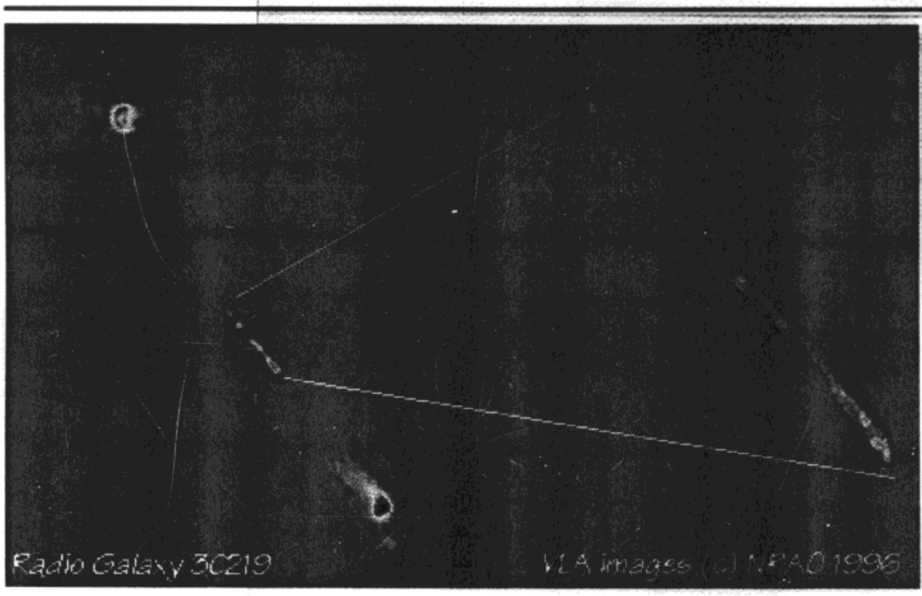

- FR II (double-lobed) radio galaxy at z=0.1745 (544/*h* Mpc, H = 100*h* km/s/Mpc)
- Filamentary outer lobes extending several hundred kpc
- Bright, extended hot spots in both lobes
- Abbreviated (restarting?) jet and counterjet
- (Left) VLA 1.4+1.6 GHz combined image at 1.4 arcsec resolution
- (Right) VLA 8 GHz image of jets at 0.1 arcsec resolution
- Ultra-compact, aligned bright knots at both jet tips
- Other images available:
  - alternate view of large scale structure
  - optical/radio montage (17k JPEG) relating radio source to host galaxy

---

For discussion of the large-scale structure, see "Origin of the structures and polarization in the classical double 3C219" by David A. Clarke, Alan H. Bridle, Jack O. Burns, Richard A. Perley & Michael L. Norman, *The Astronomical Journal*, **385**, 173-187 (1992)

For discussion of the structure in the jets, see "Fine Structure in the jets of 3C219", by Richard A. Perley, Alan H. Bridle, & David A. Clarke, in *Sub-arcsecond radio Astronomy*, eds. R.J.Davis & R.S.Booth, (Cambridge University Press), 258-260 (1994).

Also see "Collimation and polarization of the jets in 3C219", by Alan H. Bridle, Richard A. Perley, & Richard N. Henriksen, *The Astronomical Journal*, **92**, 534-545 (1986).

⬅ **Go back to:**

Radio Lobe of 3C 111

(Meisenheimer et al., Astron. Astrophys. 219, 63 (1989)

Synchrotron Radiation from accelerated e

In the radio lobes!

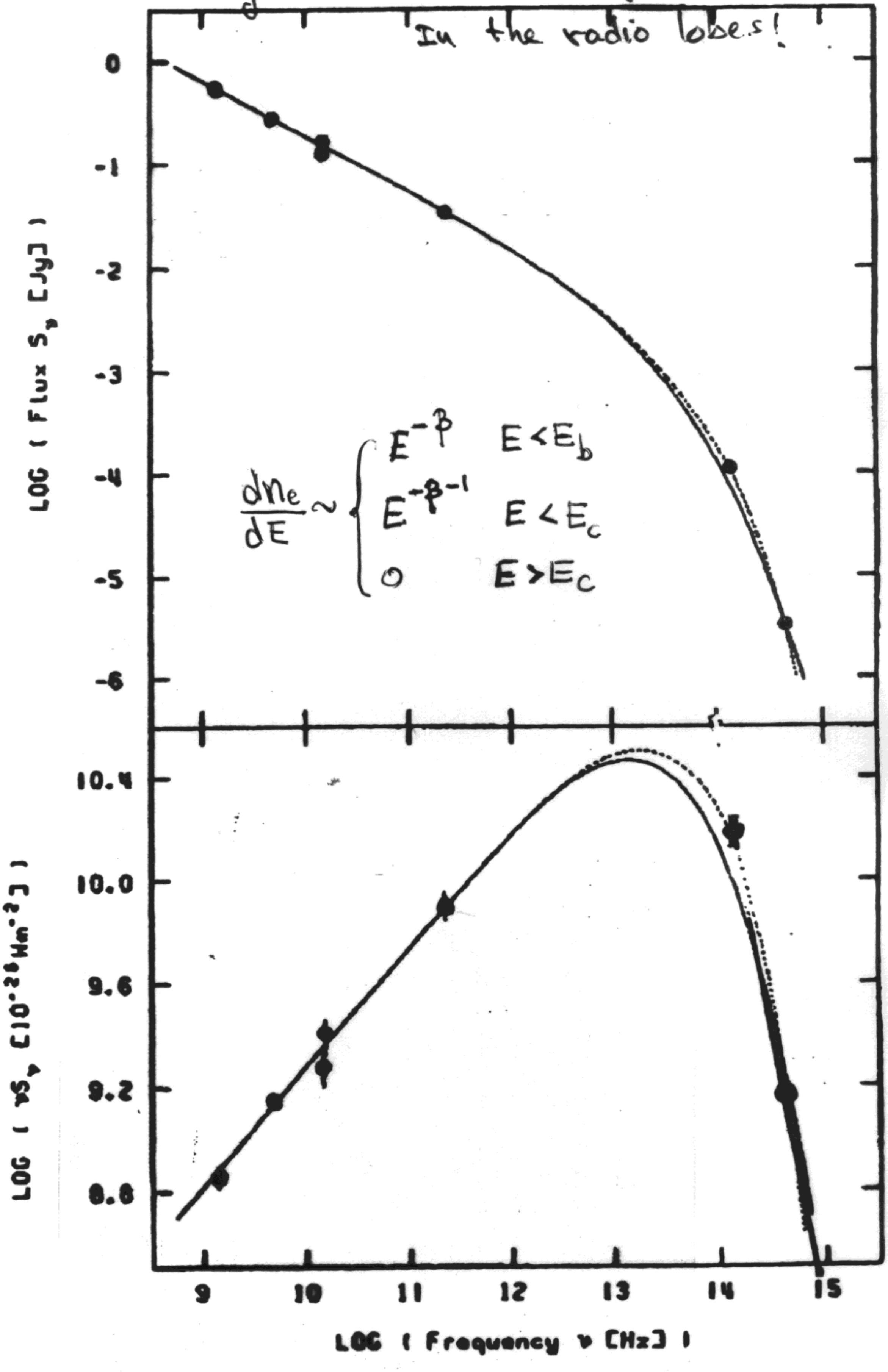

$$\frac{dn_e}{dE} \sim \begin{cases} E^{-\beta} & E < E_b \\ E^{-\beta-1} & E < E_c \\ 0 & E > E_c \end{cases}$$

Fig. 4c. Same as Fig. 4a for 3C 111 east

Two Opposite Narrowly Collimated Jets From The Quasar 3C175 Produces Radio Lobes When They stop At a Distance of ~ 200 kpc!

Quasar 3C 175

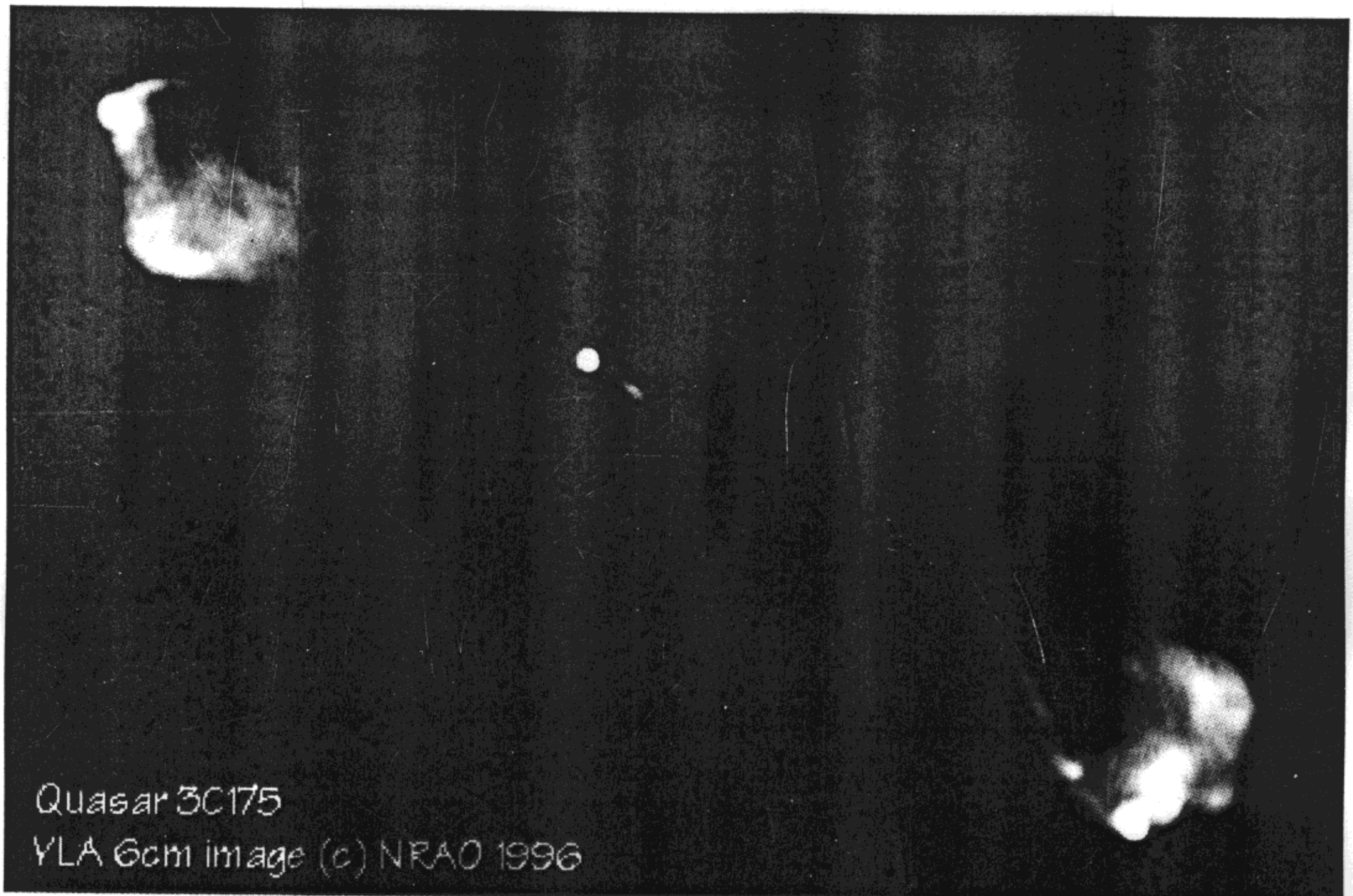

$E \sim 10^{60}$ erg!

Microqusar = Miniature Quasars

Microquasar	Nature	Jet Velocity
GRS 1915+105	SBH + High Mass *	0.92 c
GRO J1655-40	SBH + Low Mass *	0.92 c
SS433	NS + High Mass *	0.26 c
Sco-X	NS + Low Mass *	?
⋮		

GRS 1915+105 ($\ell = 45°$, $b = 0°$)

ANTI-PARALLEL EJECTION OF A TWIN PAIR OF CLOUDS MOVING AT $V = 0.92c$ AND $\theta = 70°$

VLA-A λ 3.5 cm POSITION ACCURACY 0.02"

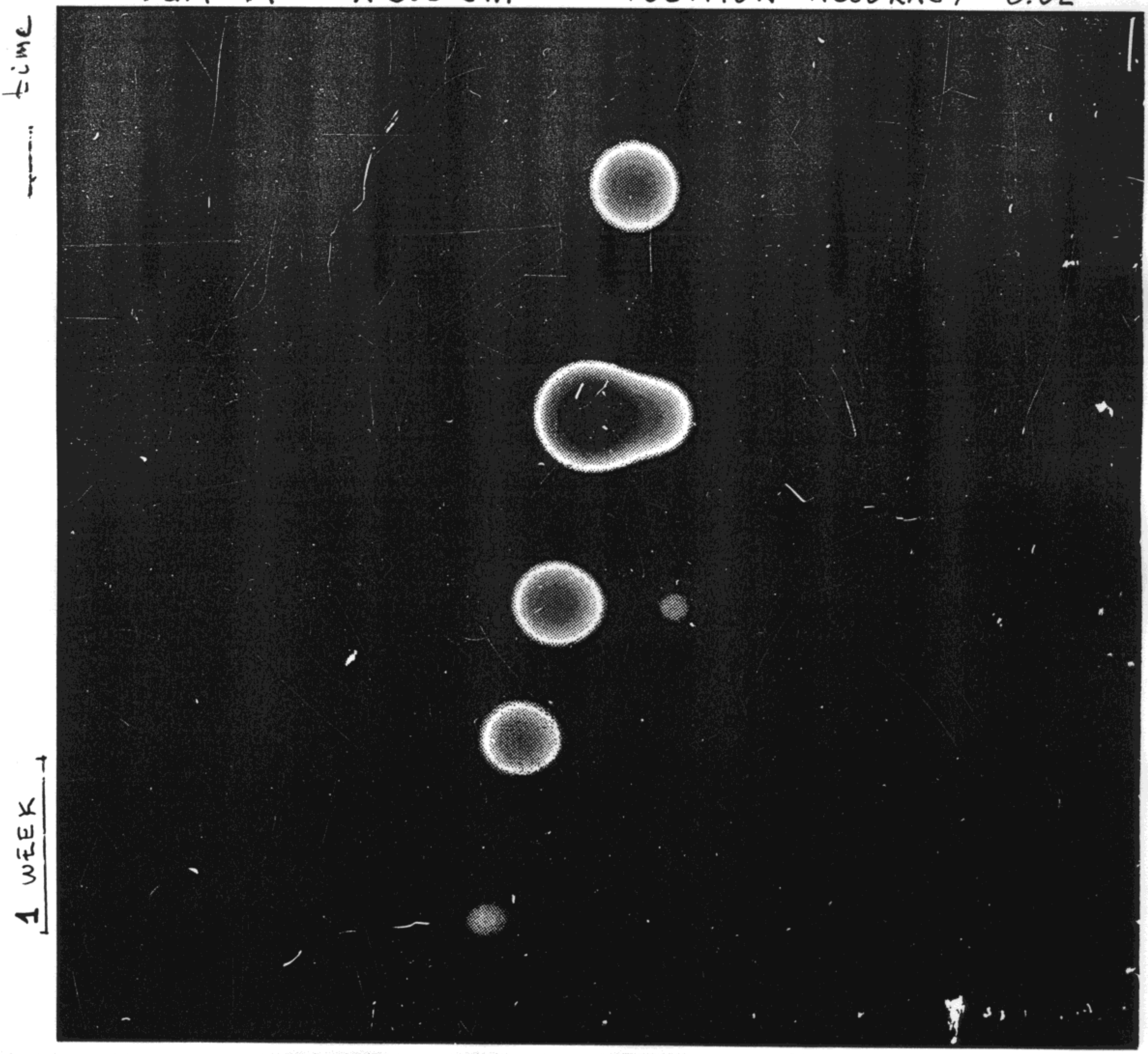

Jet Deflection

3C334 = B1618+177

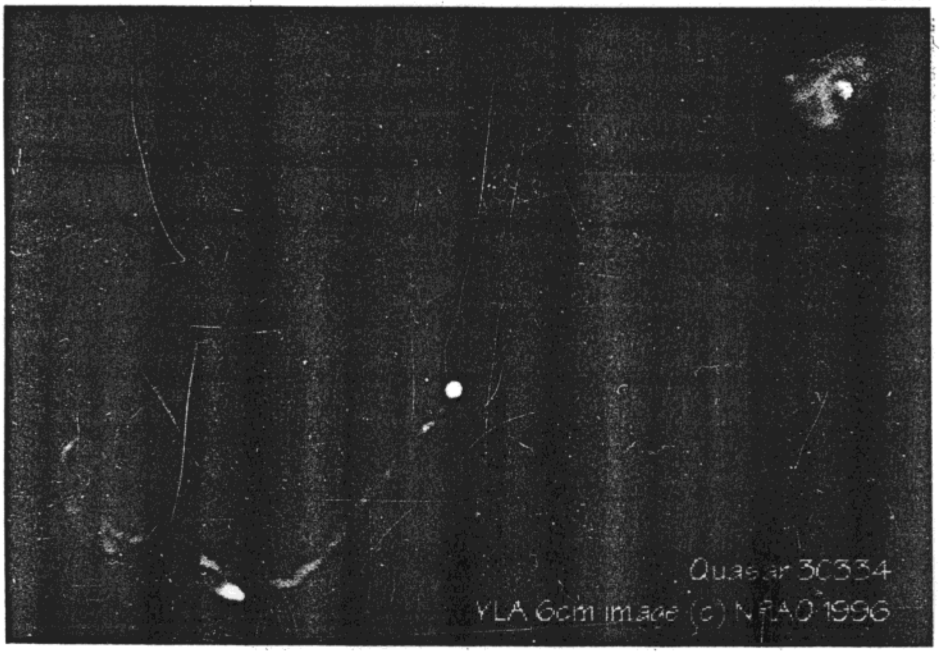

- FR II quasar at z=0.555
- Overall linear size 215/*h* kpc (Hubble constant H = 100*h* km/s/Mpc)
- Double lobes with hot spots and filaments
- Jet with possible counterjet opposite outer segment
- Jet "richochets" entering its lobe
- Superluminal motion at (1.6/*h*)c has been detected in the nuclear radio source
- VLA 4.9 GHz image at 0.35 arcsec resolution

See also Deep VLA Imaging of Twelve Extended 3CR Quasars, by Alan H. Bridle, David H. Hough, Colin J. Lonsdale, Jack O. Burns and Robert A. Laing, *The Astronomical Journal*, **108**, 766-820 (1994).

Go back to:

- Alan Bridle's Image Gallery
- Alan Bridle's Home Page
- NRAO Charlottesville Home Page
- NRAO VLA Home Page
- AstroWeb Home Page

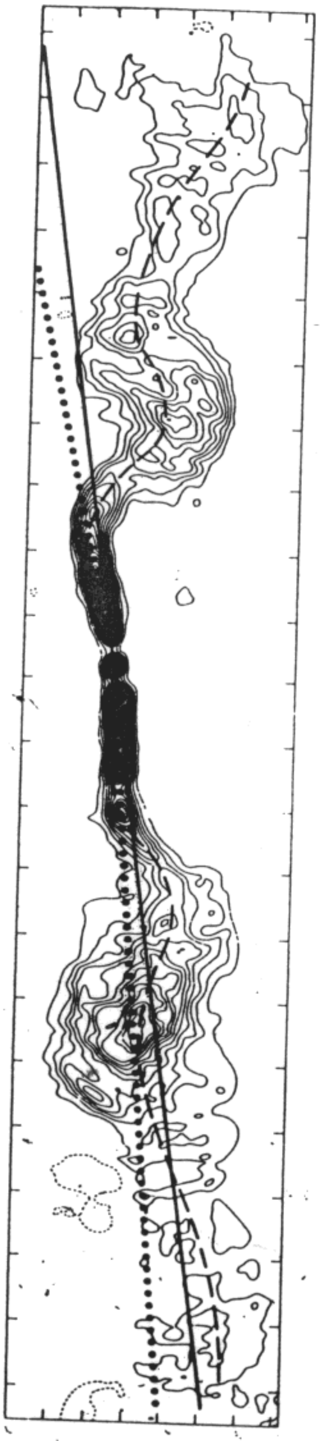

FIG. 6.—Radio map of 3C 449. The dotted lines along the opposed jet center lines inside the sharp bends lie about 4° from the straight solid line through the nucleus. The dashed lines indicate oscillation of the jet center lines beyond the sharp bends.

- Non Colinear Jets
- Deflection/Precession of Jets

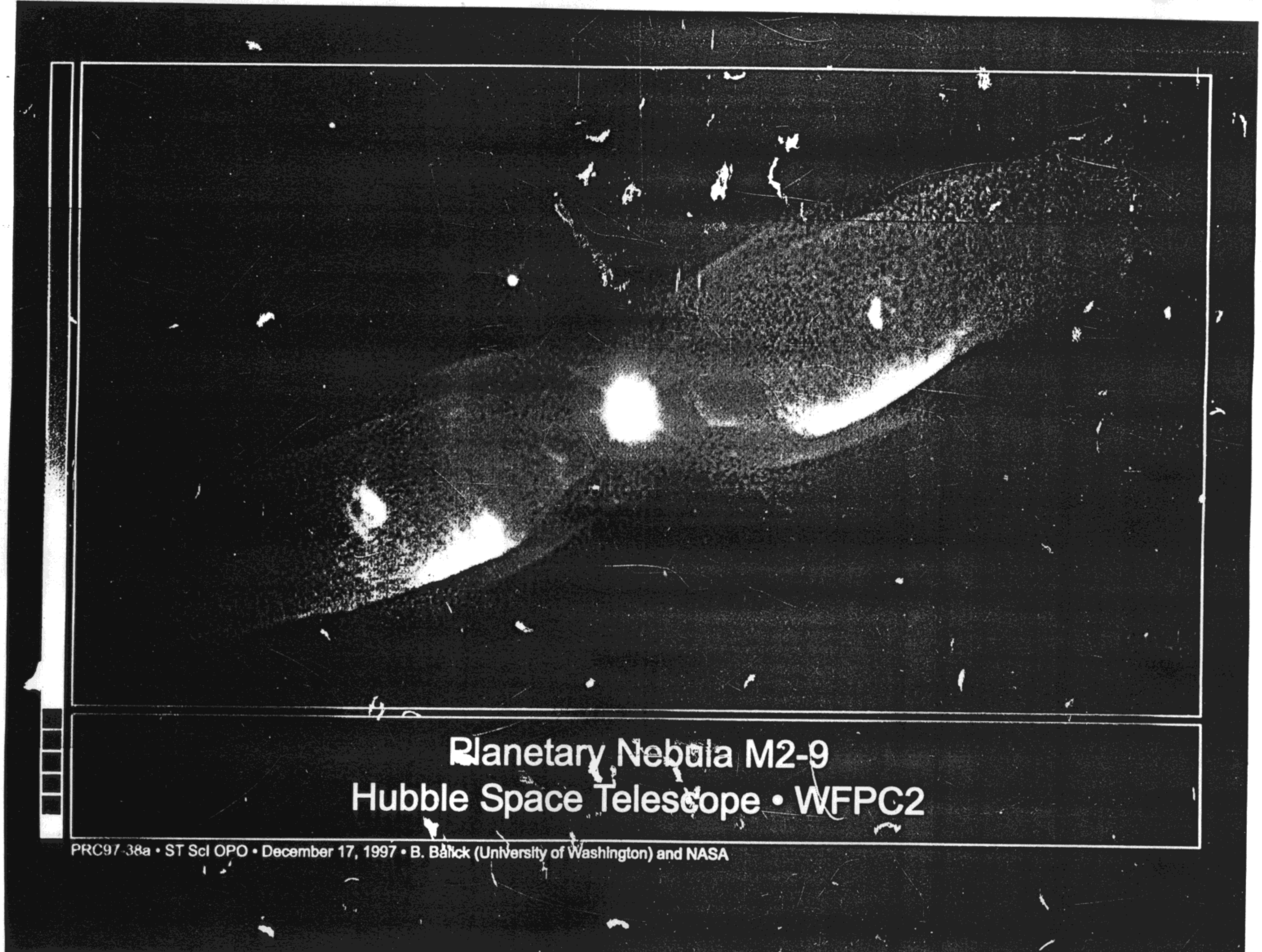
Planetary Nebula M2-9
Hubble Space Telescope • WFPC2
PRC97-38a • ST ScI OPO • December 17, 1997 • B. Balick (University of Washington) and NASA

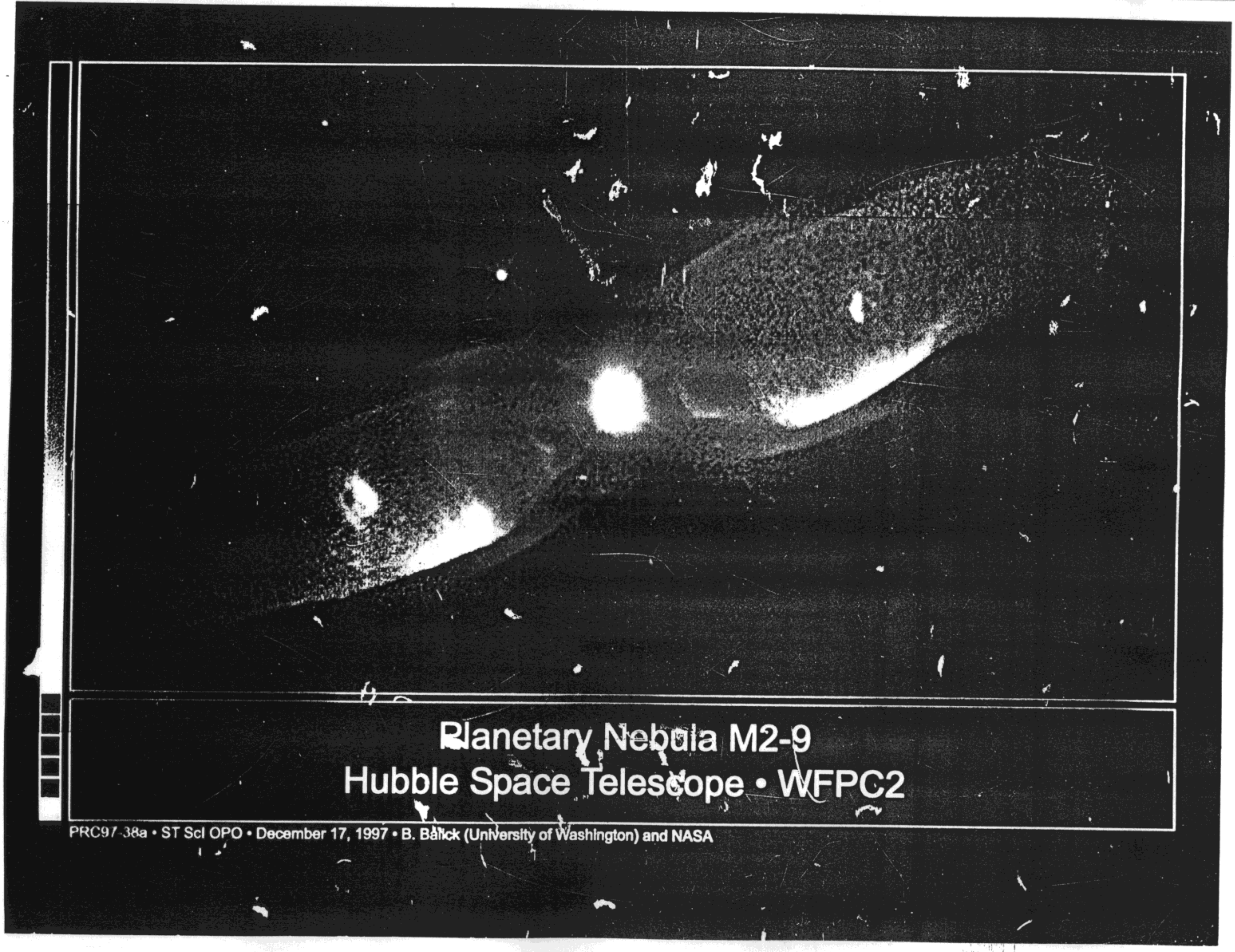
Planetary Nebula M2-9
Hubble Space Telescope • WFPC2
PRC97-38a • ST ScI OPO • December 17, 1997 • B. Balick (University of Washington) and NASA

Color Superconductivity and Chiral Symmetry Restoration at Nonzero Baryon Density and Temperature*

Jürgen Berges and Krishna Rajagopal†
Center for Theoretical Physics
Laboratory for Nuclear Science
and Department of Physics
Massachusetts Institute of Technology
Cambridge, Massachusetts 02139

See also: M. Alford, K. Rajagopal and F. Wilczek PL B 422, 227
R. Rapp et al., PRL 81, 53 (1998)
F. Wilczek, Nature 395, 220 (1998)

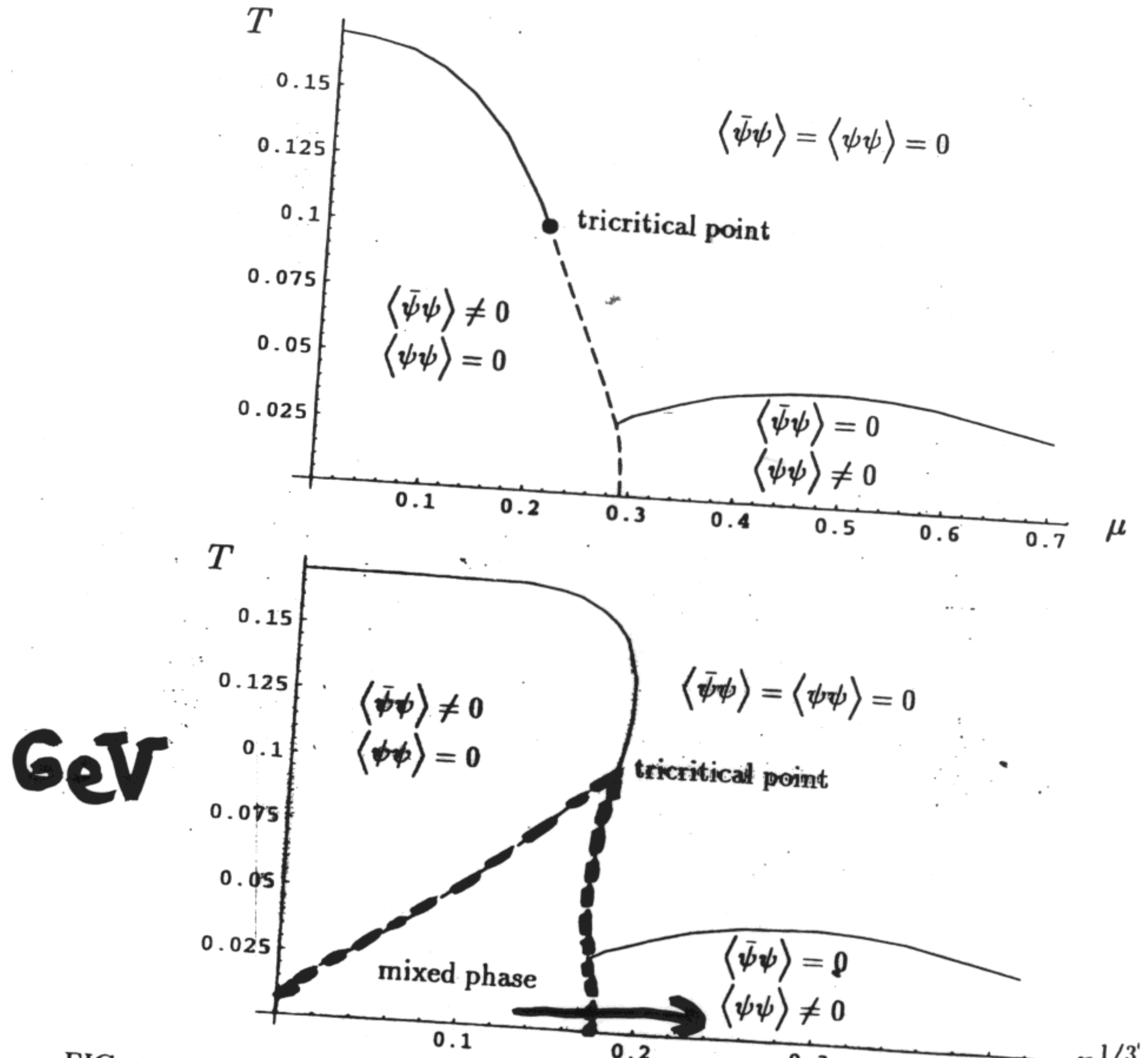

FIG. 4. Phase diagram as a function of T and μ, and as a function of T and $n^{1/3}$ ...

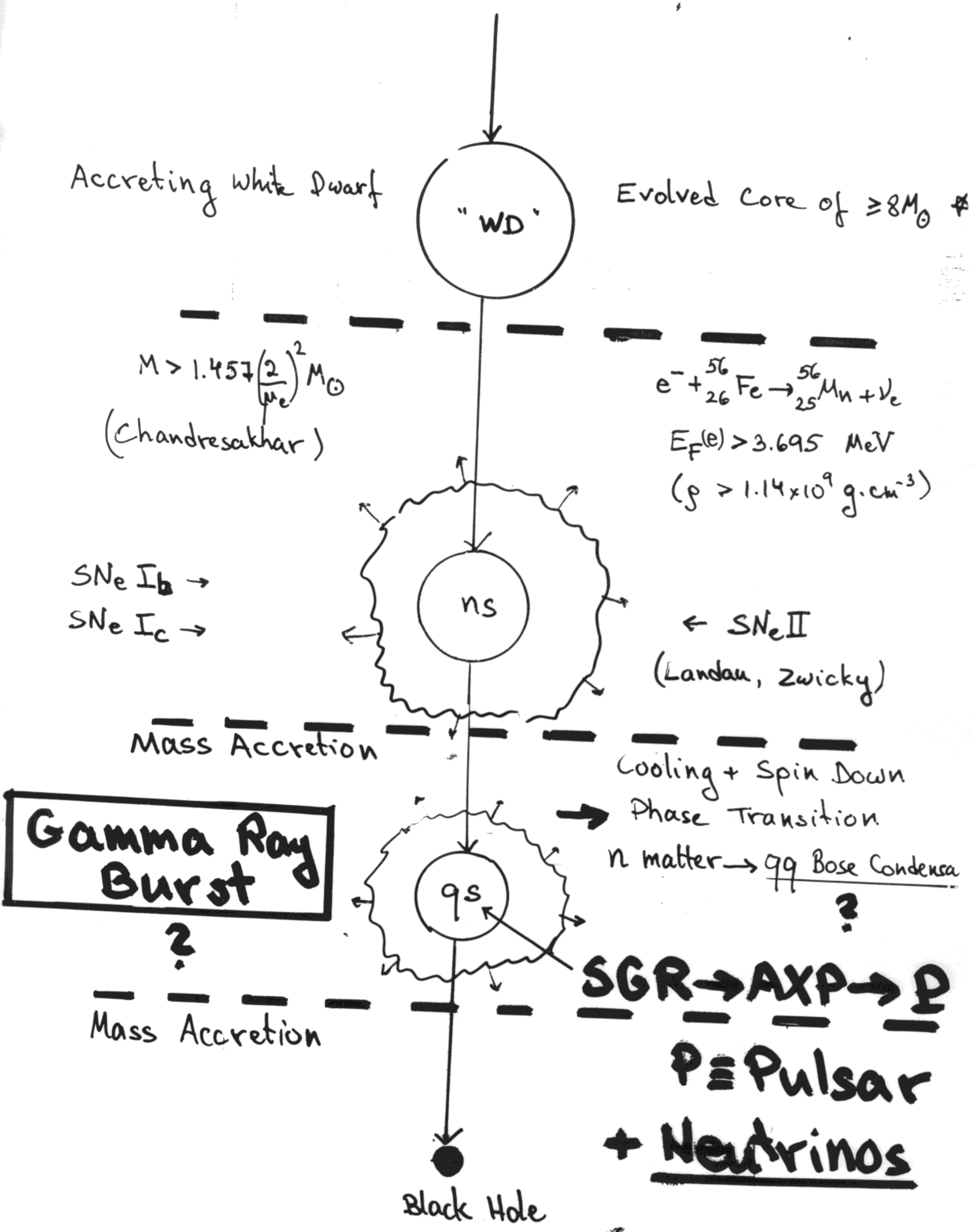
Accreting White Dwarf
"WD"
Evolved Core of $\geq 8 M_{\odot}$ ☆
$M > 1.457 \left(\frac{2}{\mu_e}\right)^2 M_{\odot}$
(Chandresakhar)
$e^- + {}^{56}_{26}Fe \rightarrow {}^{56}_{25}Mn + \nu_e$
$E_F^{(e)} > 3.695$ MeV
($\rho > 1.14 \times 10^9$ g.cm^{-3})
SNe Ib →
SNe Ic →
ns
← SNe II
(Landau, Zwicky)
Mass Accretion
Cooling + Spin Down
Phase Transition
n matter → qq Bose Condensa
?
Gamma Ray Burst
?
qs
SGR → AXP → P
P ≡ Pulsar
+ Neutrinos
Mass Accretion
Black Hole

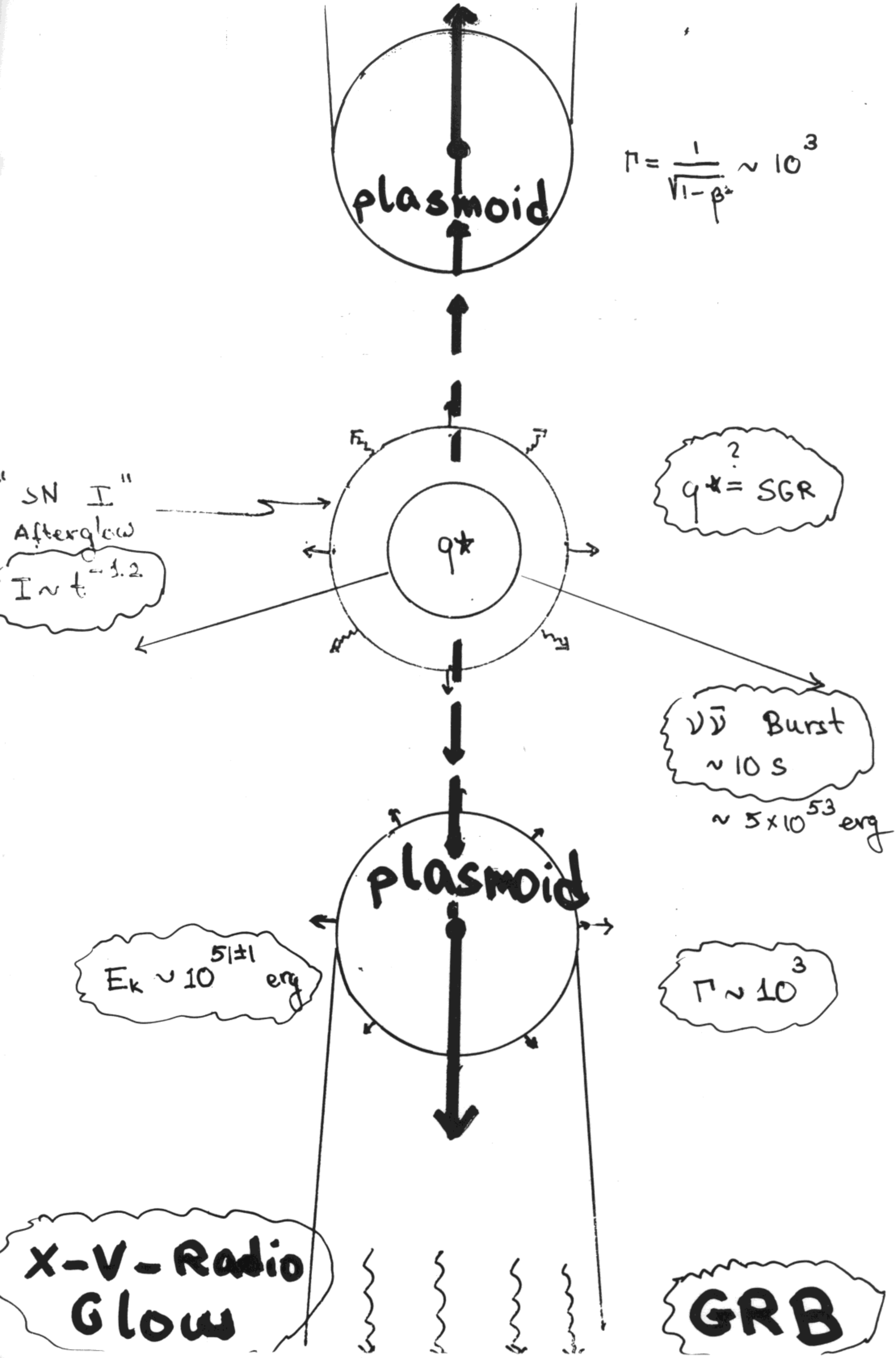
plasmoid
$\Gamma = \frac{1}{\sqrt{1-\beta^2}} \sim 10^3$
"SN I"
Afterglow
$I \sim t^{-1.2}$
q*
q* = SGR ?
$\nu\bar{\nu}$ Burst
~10 s
~ 5×10^{53} erg
plasmoid
$E_K \sim 10^{51\pm1}$ erg
$\Gamma \sim 10^3$
X-V-Radio Glow
GRB

R_{MW} [GRB]

$$R_{MW} \overset{\sim}{=} \frac{R_{UNIV}\, L_{MW} \left(R[SFR, z=0] / R[SFR, z \geq 1] \right)}{\rho_L(z=0) \int \frac{dV_c}{dz} \frac{1}{1+z}\, dz}$$

e.g.,

$\Omega = 1$

$$\int_0^{\infty} \frac{dV_c}{dz} \frac{dz}{1+z} = 16\pi \left(\frac{c}{H_0}\right)^3 \int_0^{z_\infty} \frac{\left(1+z-\sqrt{1+z}\right)^2}{(1+z)^{9/2}}\, dz = \frac{16\pi}{30} \left(\frac{c}{H_0}\right)^3$$

$$R_{UNIV}[GRB] \simeq 10^3\, y^{-1}$$

$$L_{MW} \simeq 2.3 \times 10^{10} L_\odot$$

$$\rho_L(z=0) \simeq 1.8h \times 10^8 L_\odot\, Mpc^{-3}$$

$$\frac{R(SFR, z \geq 1)}{R(SFR, z=0)} \simeq 15$$

$$\Rightarrow \boxed{R_{MW}[GRB] \simeq 2 \times 10^{-8}\, y^{-1}}$$

No. of Observable GRBs
In the Milky Way Galaxy per year

Star Formation Rate (SFR)

(C.C. Steidel et al.

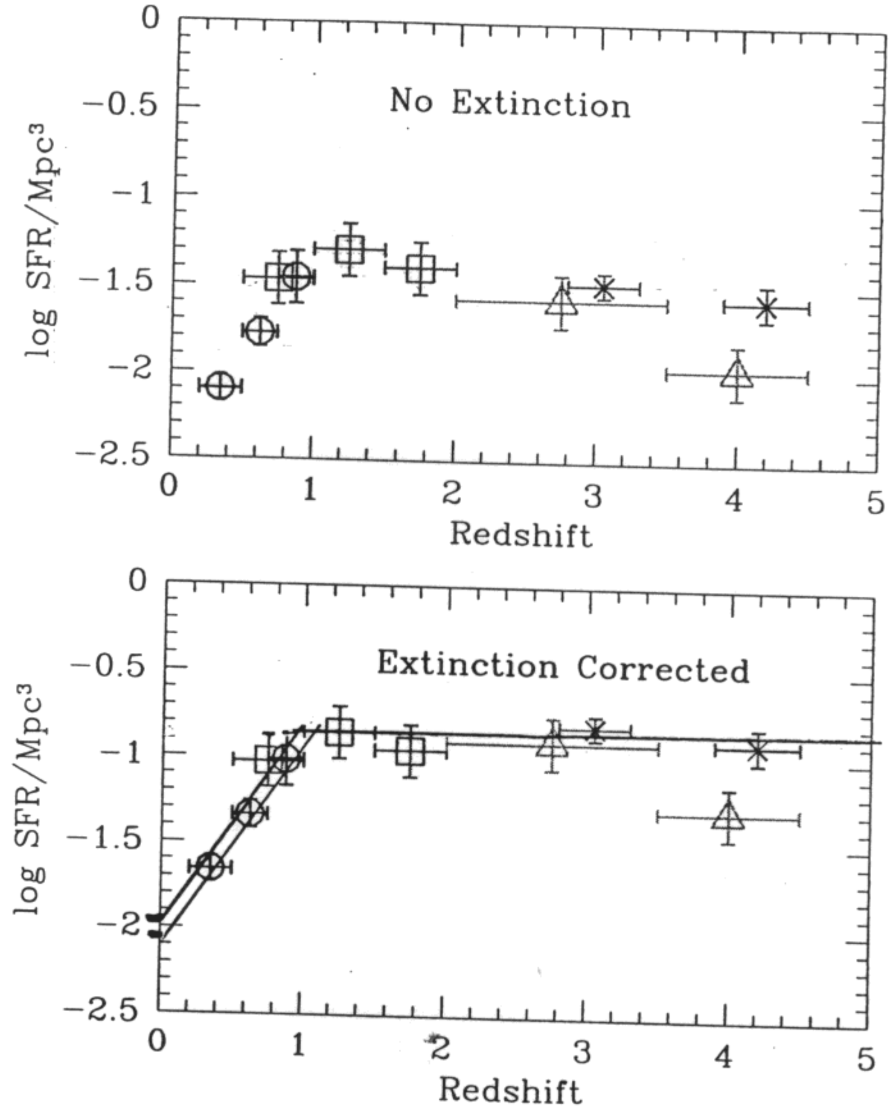

Fig. 9.— The UV luminosity density as a function of redshift, following Madau *et al.* 1996 (also using $H_0 = 50$ km s^{-1}Mpc^{-1} and $q_0 = 0.5$, for consistency). The different points come from Lilly *et al.* (1996) [circles], Connolly *et al.* (1997) [squares], and Madau *et al.* 1997 (triangles). The new points from this work are shown as crosses. See text for details.)

New **Data From :**

Imaging :

Palomar : 200-inch Hale Tel

Cerro-Tololo Inter Am: 4 m

William Herschel Telescope.

Spectroscopy :

Keck II : 10 m telescope

$$\Gamma = ?$$

$$\dot{N}_{GRB} \cong 10^{3}\, y^{-1} / \text{Universe}$$

$$\Rightarrow \dot{N}_{GRB}[MW] \approx 10^{-8}\, y^{-1}$$

$$\dot{N}_{GRB}[MW] \cong 2\,\frac{\Delta\Omega}{4\pi}\,\dot{N}_{NS}[MW]$$

$$\approx 2\times 10^{-2}\, y^{-1}$$

$$\Delta\Omega = \pi\theta_b^2 \approx \pi/\Gamma^2$$

$$\Rightarrow \Gamma^2 \cong (1/2)\,\dot{N}_{NS}/\dot{N}_{GRB} \approx 10^{6}$$

$$\Rightarrow \boxed{\Gamma \approx 10^{3}}$$

If the kick velocity of NS (at birth) is due to jet ejection:

$M_{NS} \sim 1.4\, M_\odot$

$\langle V \rangle \sim 450 \pm 90$ km·s^{-1}

$v \sim c$; $\Gamma >> 1$

From momentum conservation:

$$P_{jet} = M_{NS} V$$

$$E_{jet} \simeq c P_{jet} \simeq M_{NS} c V \sim 4 \times 10^{51} \text{ erg}$$

If two opposite jets are ejected $\Delta E_{jets} \sim 4 \times 10^{51}$

$$\Rightarrow \boxed{E_{jet} \gtrsim 10^{52} \text{ erg}}$$

(Birth of NS releases $E_b \sim \frac{GM^2}{R} \sim 5 \times 10^{53}$ erg)

(Phase transition in NS releases

$$\Delta E \sim \frac{GM^2}{R} \frac{\Delta R}{R} \sim 5 \times 10^{53} \frac{\Delta R}{R} \text{ erg} \quad)$$

(Accretion of NS onto BH releases

$$\Delta E \sim M_{NS} c^2 \sim 2.5 \times 10^{54} \text{ erg} \quad)$$

Relativistic Jet Boosting Starlight

(N. Shaviv + A. Dar, 1995)

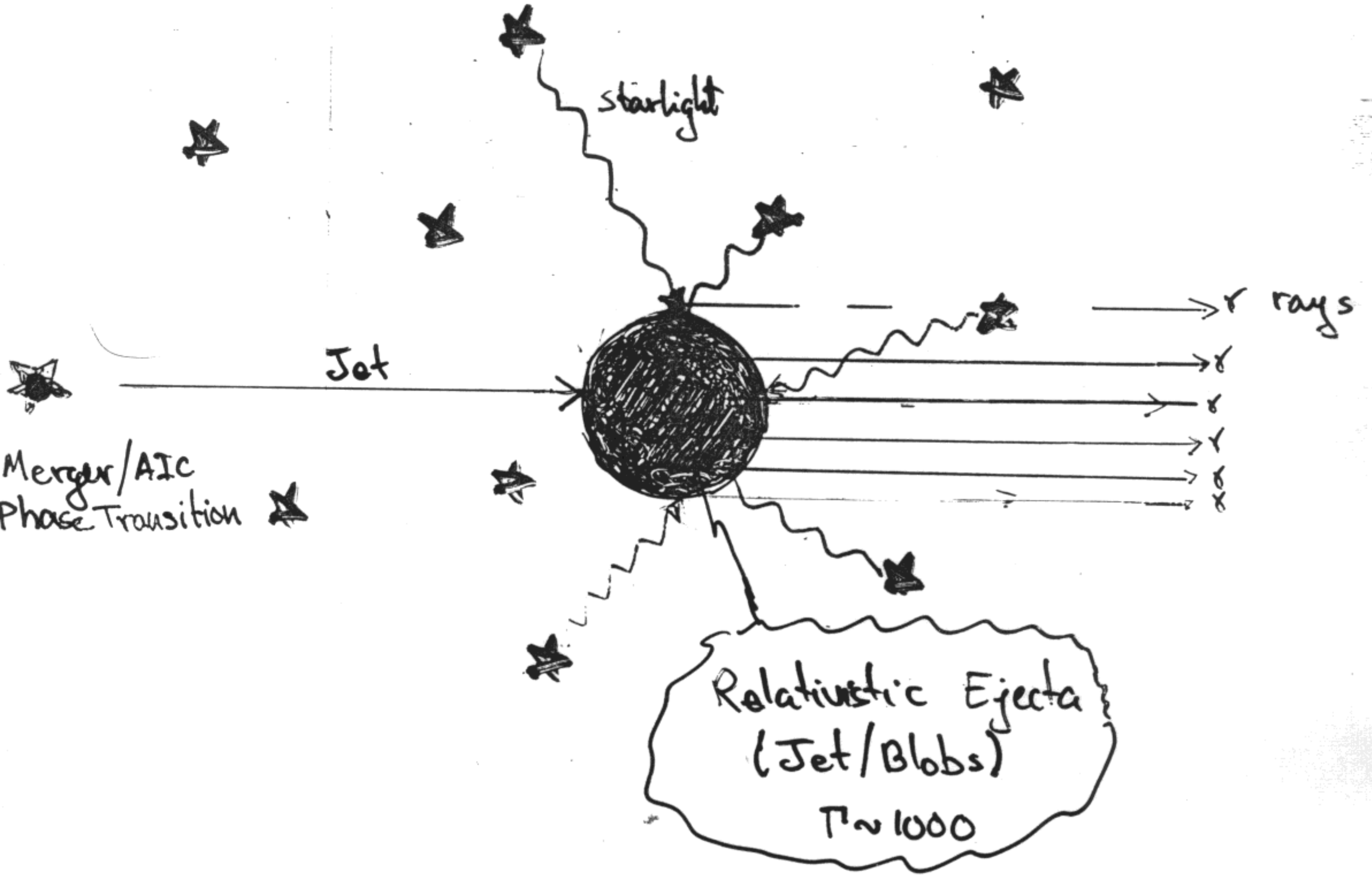

The "reflected" starlight ($\varepsilon \sim 1$ eV)
is beamed ($\theta \lesssim 1/\Gamma$) and boosted ($\varepsilon \to \varepsilon\Gamma^2 \sim$ MeV)

by:

- Inverse Compton scattering $\sigma_T \lesssim 10^{-24}\ \mathrm{cm}^2$
- Photoexcitation / Photoemission $\sigma_{ex} \gtrsim 10^{-18}\ \mathrm{cm}^2$!

Dermer 1997: Synchrotron Emission from plasma blobs

(I)

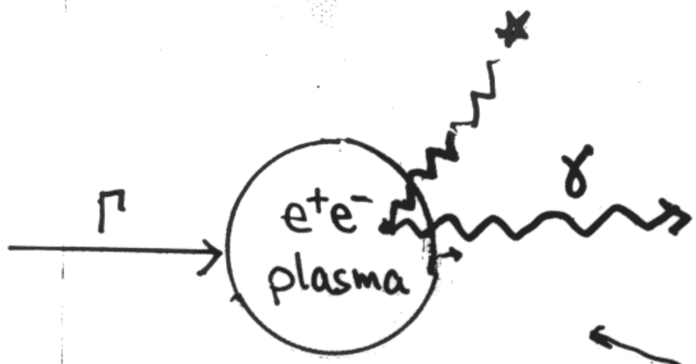

Stellar Light Scattered by Inverse Compton
To ~ MeV energy

$$\langle E_\gamma \rangle \cong \Gamma^2 \varepsilon_\gamma / (1+z) \simeq \frac{\Gamma_3^2 \varepsilon_{eV}}{1+z} \; \mathrm{MeV}$$

$$n_\gamma \cong \frac{N_e \sigma_T N_\gamma}{D^2 \Delta\Omega} \sim \frac{E_{52} N_{22} \Gamma_3}{D_{29}^2} \; 2.5 \quad \mathrm{cm}^{-2}$$

$\Delta\Omega = \pi/\Gamma^2$

(II)

Photoabsorption/emission of light by heavy metals
(CR composition $N_h \sim 10^{-2} N_H$)
(Doppler shifted $L\alpha$ and K_α (Fe) were detected from the jets of SS433)

$$n_\gamma \cong \frac{N_h \sigma_a N_\gamma}{D^2 \Delta\Omega} \sim \frac{E_{52} \sigma_{-18} N_{22} \Gamma_3}{D_{29}^2} \; 20 \quad \mathrm{cm}^{-2}$$

$$E_\gamma \cong \Gamma \varepsilon_x / (1+z) \sim \Gamma_3 (\varepsilon_x / \mathrm{keV}) / (1+z) \; \mathrm{MeV}$$

Numerical Simulations

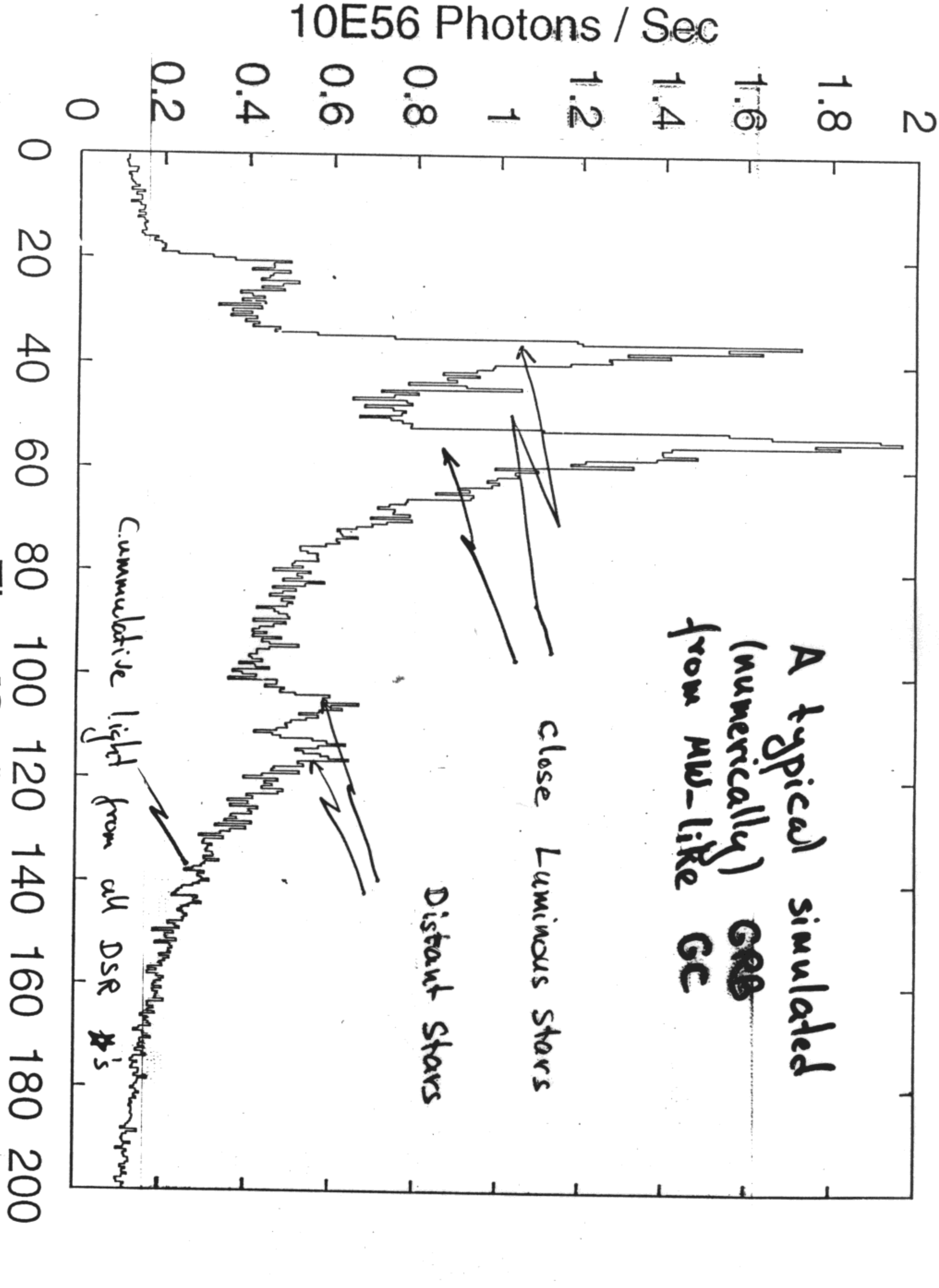

III

Overtaking Collisions

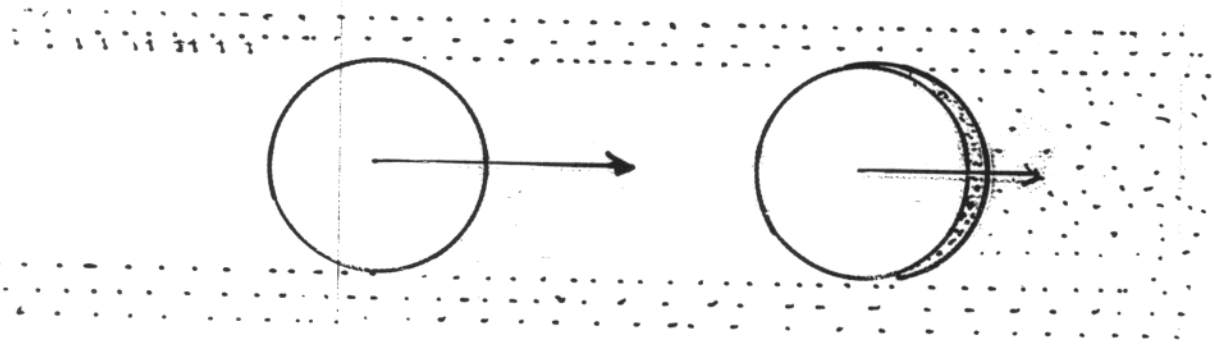

Leading Blob "Sweeps Up" The ISM and Decelerates. Later Ejected Blobs Collide With Leading Blob.

$\Rightarrow$ $\boxed{\text{Emission Of Synchrotron Radiation}}$?

Synchrotron cooling cuts off electron acceleration at

$$\Gamma_e \sim 7\times10^{7}\,(B/G)^{-1/2}$$

Typical synchrotron γ emission energy

$$E_\gamma \sim 1.3\times10^{-8}\,\Gamma_e^2\,\Gamma\,(B/G) \sim 7\times10^{10}\,\Gamma_3 \text{ eV !}$$

(Why peak energy is $E_p \sim 0.1 - 1.0$ MeV ?)

From Energy/Momentum Conservation :

$$\gamma(R{=}0)=\Gamma \;; \qquad \gamma = \frac{\Gamma}{1+R/R_0} \quad \text{i.e.,} \qquad R = R_0\,(\Gamma/\gamma - 1)$$

Distance From Ejection Point

where $$R_0 \equiv \frac{E_k}{n m_p c^2 \Gamma S} \cong \frac{E_{52}}{n\,\Gamma_3 (R/0.01\,pc)^2}\, 2.2\times10^{18} \text{ cm}$$

$$t_{obs} = \left(\frac{R_0}{6c\Gamma^2}\right)\left[\left(\frac{\Gamma}{\gamma}\right)^3 - 1\right]$$

JETTED AFTERGLOWS

Synchrotron and Inverse Compton Afterglows

(See Chiang and Dermer 1997 For Detailed Numerical Simulations)

$$I_\nu \sim I_0 \nu^{-\frac{p-1}{2}} \gamma^{3+\frac{p-1}{2}}$$

$$t_{ob} = (R_0/6c\Gamma^2)\left[(\Gamma/\gamma)^3 - 1\right] \sim \gamma^{-3}$$

$$\Rightarrow \quad I_\nu \sim I_0 \nu^{-\frac{p-1}{2}} (t+t_0)^{-1-(p-1)/6}$$

since $\quad p = 2.5 \pm 0.5$

meV, eV, keV

$$\Rightarrow I_\nu \sim I_0 \nu^{-\underline{0.75\pm0.25}} (t+t_0)^{-\underline{1.25\pm0.08}}$$

GeV γ-Rays and TeV neutrinos

$$pp \to \pi^0 X, \quad \pi^0 \to 2\gamma \qquad pp \to \pi^\pm X, \quad \pi^\pm \to \mu\nu_\mu, \quad \mu \to e\nu_e\nu_\mu$$

$$p\gamma \to \pi^0 X, \quad \pi^0 \to 2\gamma \qquad p\gamma \to \pi^\pm X$$

$$I_\gamma \sim g\sigma_{in} N_H I_p \; ; \; g = 0.195 \exp[-3.84(p-2) + 1.22(p-2)$$

$$F_\gamma(>100\,\mathrm{MeV}) \approx \frac{E_{52} N_{22} \Gamma_3^2}{D_{29}^2} \times 10^{-5}\ \mathrm{erg \cdot cm^{-2}}$$

$$F_{\nu_\mu}(>100\,\mathrm{MeV}) \approx \frac{E_{52} N_{22} \Gamma_3^2}{D_{29}^2} \times 10^{-5}\ \mathrm{erg \cdot cm^{-2}}$$

High Column Density Radiation Field

High Column Density Gas Targets:

Interstellar gas in star burst regions, stellar winds, ... Envelopes

HE COSMIC RAYS

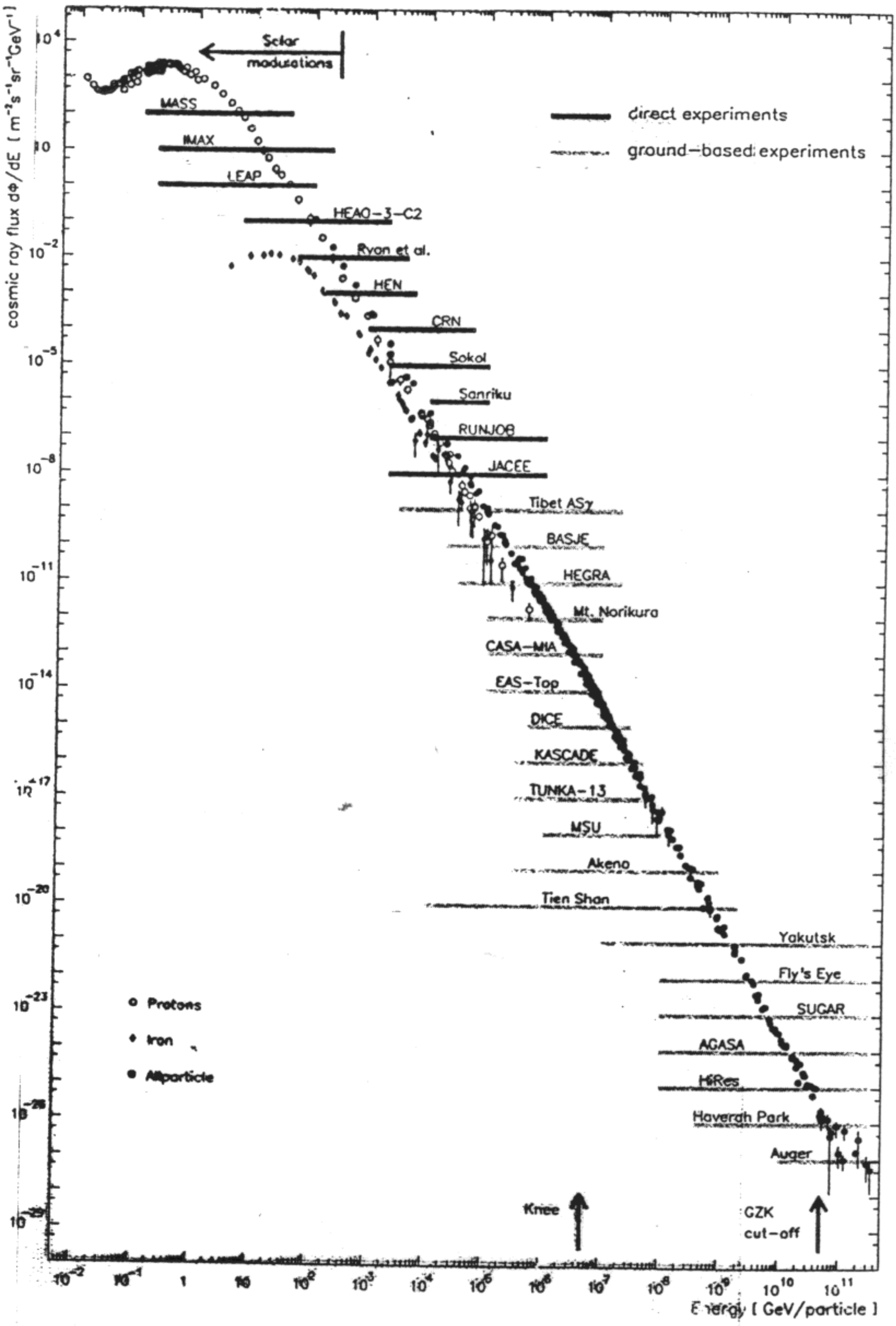

Figure 1: The energy ranges of several direct and indirect experiments, which provided data on the cosmic ray spectrum or will provide data in the near future.

THE CURRENT PARADIGM :

CR WITH $E < E_{KNEE} \sim 10^{15.5}$ eV

ACCELERATED IN SNR

CR WITH $E > E_{KNEE}$

GALACTIC OR EXTRAGALACTIC IN ORIGIN

CR WITH $E > E_{ANKLE} \sim 10^{18.5}$ eV

EXTRAGALACTIC IN ORIGIN *

* Gyration Radius (Larmor Radius) :

$$R_L = \frac{E}{zeB_\perp} \sim 3.1\times10^{15}\left(\frac{E}{10^{18}\,eV}\right)\left(\frac{ZB_\perp}{Gauss}\right)^{-1} \text{ cm}$$

If Coherence Length of B is $\lambda \ll R_L$:

$$\Delta\theta \simeq \frac{\lambda_c}{R_L} \simeq 0.52^\circ\, Z\left(\frac{E}{10^{20}\,eV}\right)^{-1}\left(\frac{\lambda}{kpc}\right)\left(\frac{B_\perp}{\mu G}\right)$$

Accumulated Deflection when $\theta \ll 1$ (rad) :

r.m.s.

$$\theta_{ac} \simeq 5.4^\circ \underbrace{\left(\frac{d}{50\,kpc}\right)^{1/2}}_{R_h} \underbrace{\left(\frac{\lambda}{1\,kpc}\right)^{1/2}\left(\frac{ZB}{3\mu G}\right)}_{\text{Faraday Rotaion}} \left(\frac{E}{10^{20}\,eV}\right)^{-1}$$

$$\boxed{\theta \sim \pi \quad \text{FOR} \quad E \sim 3\times10^{18}\ eV}$$

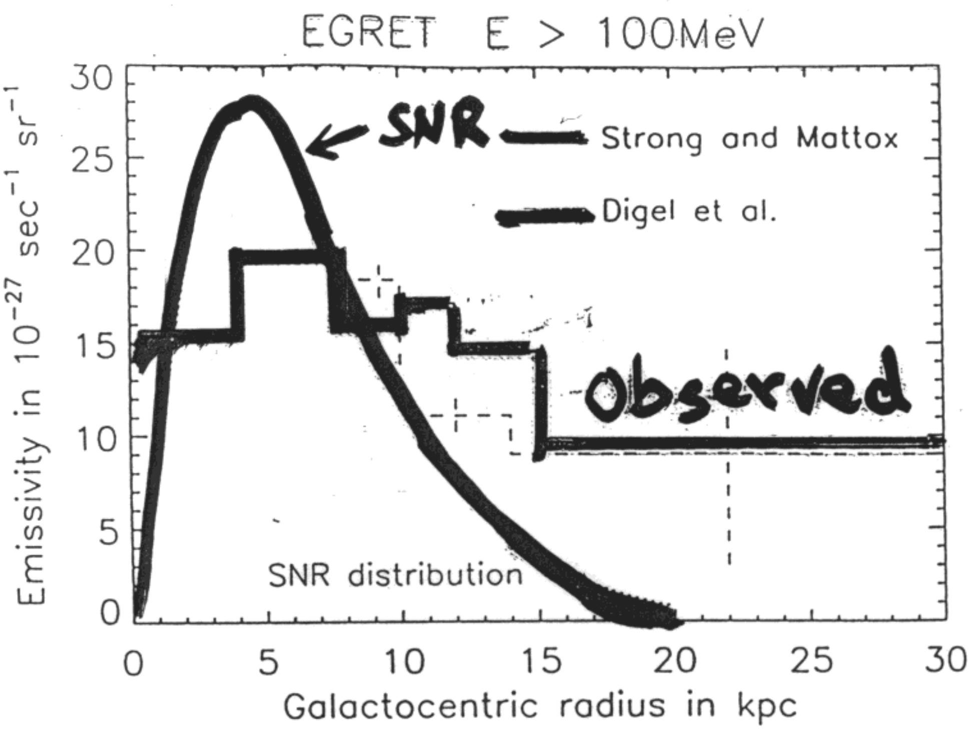

FIGURE 1. A comparison between the γ-ray emissivity gradient (solid histogram) to the distribution of SNR as possible acceleration sites (dotted line). The statistical uncertainties of the gradient are typically below 10%. The obvious discrepancy implies that either SNR are not accelerating the bulk of GeV cosmic rays, or diffusive reacceleration is operative, or galactic cosmic rays are confined on a scale of many kpc's. Please note that locally derived emissivities (dashed histogram) can differ significantly from the global trend.

Galactic γ- rays production by cosmic rays :

1. $pp \to \pi^0 X$; $\pi^0 \to 2\gamma$ photoproduction
2. $e + \gamma_{BKG} \to e' + \gamma$ Inverse Compton Scattering of BKG γ
3. $e + B \to e' + \gamma + B$ Synchrotron Radiation
4. $e + p \to e' + \gamma + p$ Bremstrhalung

$\Rightarrow$ **SNR ORIGIN OF CRs :**

Cannot explain Galactic Emissivity Gradient

Predicts CR unisotropy Above 100 TeV $> 10^3$ than Observational Limit

Highly Relativistic Jets As,

$\boxed{\text{Magnetic Mirror (Fermi) Accelerators of Cosmic Rays}}$

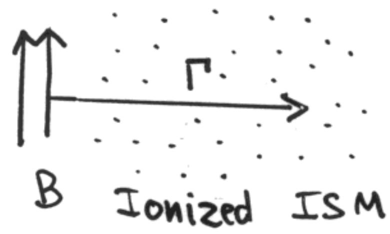

LAB FRAME

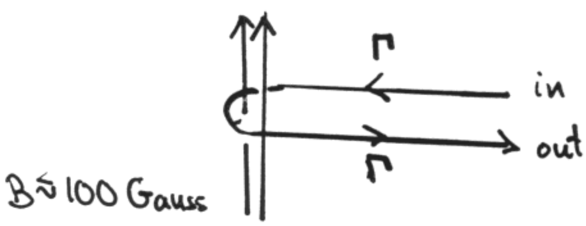

JET REST FRAME

$\Rightarrow$ REFLECTED PARTICLES HAVE LAB ENERGY

$$\boxed{E_L = 2mc^2\Gamma^2 \cong 2A\Gamma_3^2 \ PeV}$$

$$\left(R_L \lesssim 3.4\times 10^{15} (E/10^{18}\, eV)\, Z (B/G)^{-1}\ cm \ll R_{Jet} \right)$$

For n reflections:

$$E_L = 2^n mc^2 \Gamma^{2n}$$

From energy-momentum conservation:

Source Spectrum

$$\frac{dn}{dE} \sim E^{-2+1/2n} \sim \begin{cases} E^{-1.5} & n=1 \\ E^{-1.75} & n=2 \\ E^{-2} & n=\infty \end{cases}$$

$(E < mc^2\Gamma^{2n})$

Synchrotron cut-off:

$E < E \sim \Gamma A^2 Z^{-3/2} (B/G)^{-1/2}\, 10^{20}\ eV$

① WIDE Sky DISTRIBUTION

② Clustering of UHECR

③ No GZK Cutoff !!!

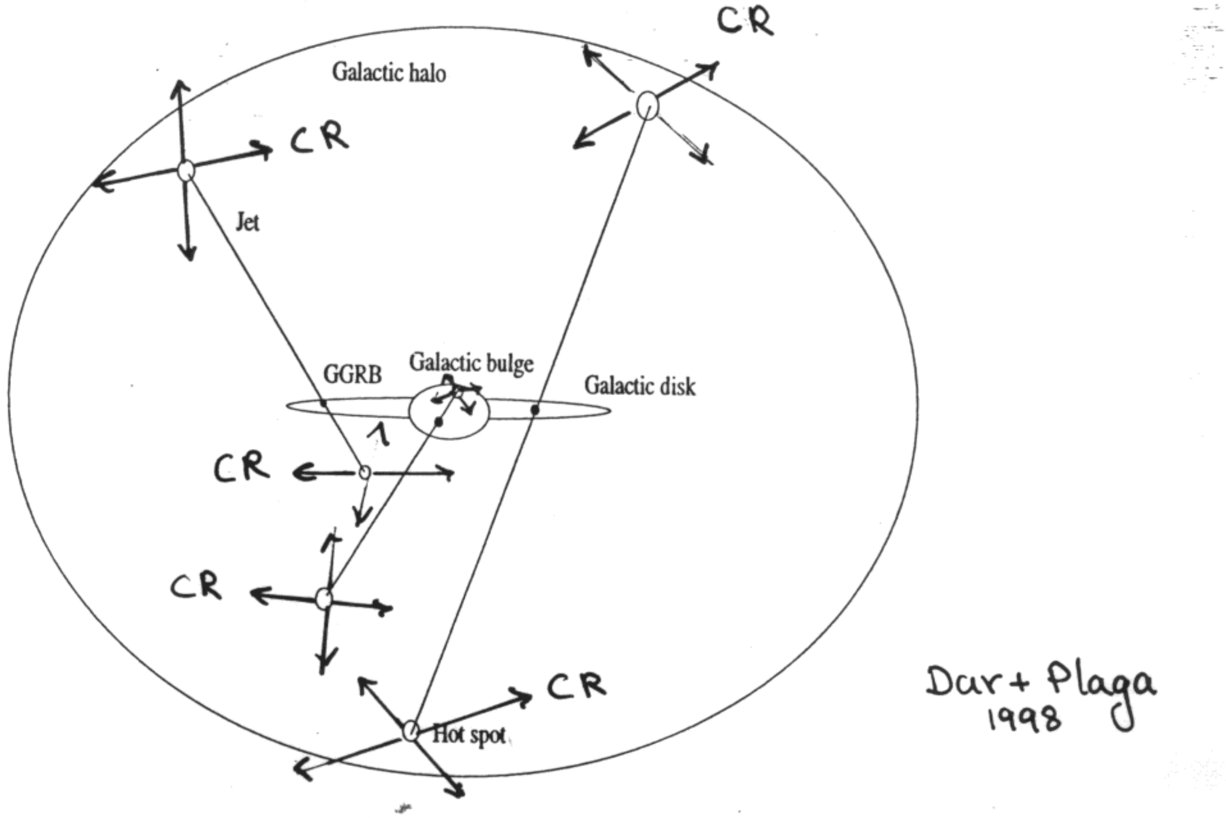

Figure 1: *A highly schematic sketch of our framework. The formation of a compact object in the disk of our Galaxy leads to an ejection of two unbalanced jets that produce "hot spots" when they stop in an extended halo.*

Dispersion in arrival direction/time due to random walk in the halo magnetic fields:

$$\Delta\theta \simeq 5.4^\circ \left(\frac{d}{50\,\mathrm{kpc}}\right)^{1/2} \left(\frac{\lambda}{1\,\mathrm{kpc}}\right)^{1/2} \left(\frac{ZB}{3\,\mu G}\right) \left(\frac{E}{10^{20}\,\mathrm{eV}}\right)^{-1} \quad \text{(r.m.s}$$

$$\Delta t \simeq \frac{d\theta^2}{2c} \simeq 750\,y \left(\frac{d}{50\,\mathrm{kpc}}\right) \left(\frac{\lambda}{\mathrm{kpc}}\right) \left(\frac{ZB}{3\,\mu G}\right)^2 \left(\frac{E}{10^{20}\,\mathrm{eV}}\right)^{-2} \quad \text{r.m}$$

IF UHECR $Z > 1$ Nuclei $\Delta\theta \propto Z$; $\Delta t \propto Z^2$!

average number of sky positions: $R_{NS}\,\Delta t \sim 60$ for $Z = 2$

OBSERVED GALACTIC SPECTRUM

Due to Magnetic Trapping

$$\frac{dn}{dE} = \tau_R \left(\frac{dn}{dE}\right)_{\text{source}}$$

From measured isotopic abundances in CR:

$$X = \int \rho\, dx \cong c\,\tau_R(E)\,\bar{\rho} = 6.9\,(E/20Z\,\text{GeV})^{-0.6}\ \text{gm}\cdot\text{cm}^{-2}$$

$$\tau_R(E) \simeq \begin{cases} \dfrac{R_h}{c} \simeq 1.6\times10^5\,(R_h/50\,\text{kpc}) & E \gtrsim E_{ankle} \\[2ex] \dfrac{R_h}{c}\left(\dfrac{E}{E_{ankle}}\right)^{-0.6} & E \lesssim E_{ankle} \end{cases}$$

"Free" escape when:

$$R_L \cong \left(\frac{E}{10^{18}\,\text{eV}}\right)\left(\frac{ZB}{3\mu G}\right)^{-1} \text{kpc} \gtrsim \lambda_c$$

Larmor Radius

coherence length of halo magnetic fields

$$\Rightarrow \quad \boxed{E \gtrsim E_{ankle} = (E/\text{EeV})\,(ZB/3\mu G)^{-1} \times 3\times10^{18}\ \text{eV}}$$

$$\frac{dn}{dE} \cong \begin{cases} C\,(E/E_{knee})^{-2.7} & ; \quad E < E_{knee} \\ C\,(E/E_{knee})^{-3.0} & ; \quad E > E_{knee} \\ C\left(\dfrac{E_{ankle}}{E_{knee}}\right)^{-3}\left(\dfrac{E}{E_{ankle}}\right)^{-2.5} & ; \quad E > E_{ankle} \end{cases}$$

ACCRETION AND COLLAPSE JETS AS COSMIC RAY ACCELERATORS

Also:

- JETS TRANSPORT GRB ENERGY TO HALO
- TRANSPORTED ENERGY PRODUCE $\sim 1\ \mu G$ HALO MAGNETIC FIELD
- ADDITIONAL ACCELERATION/ISOTROPIZATION OF Cosmic Rays In The Hot Spots.

Magnetic Trapping Enhances The Density of Galactic Cosmic Rays by

$$\frac{dn}{dE} = \tau(E)\left(\frac{dn}{dE}\right)_{source}$$

$$\boxed{\tau(E)/(R/c) = c\tau/R \sim E^{-0.6}}$$

Inferred from chemical abundance

Residence time of CR

Free escape time

observed for solar plasmas

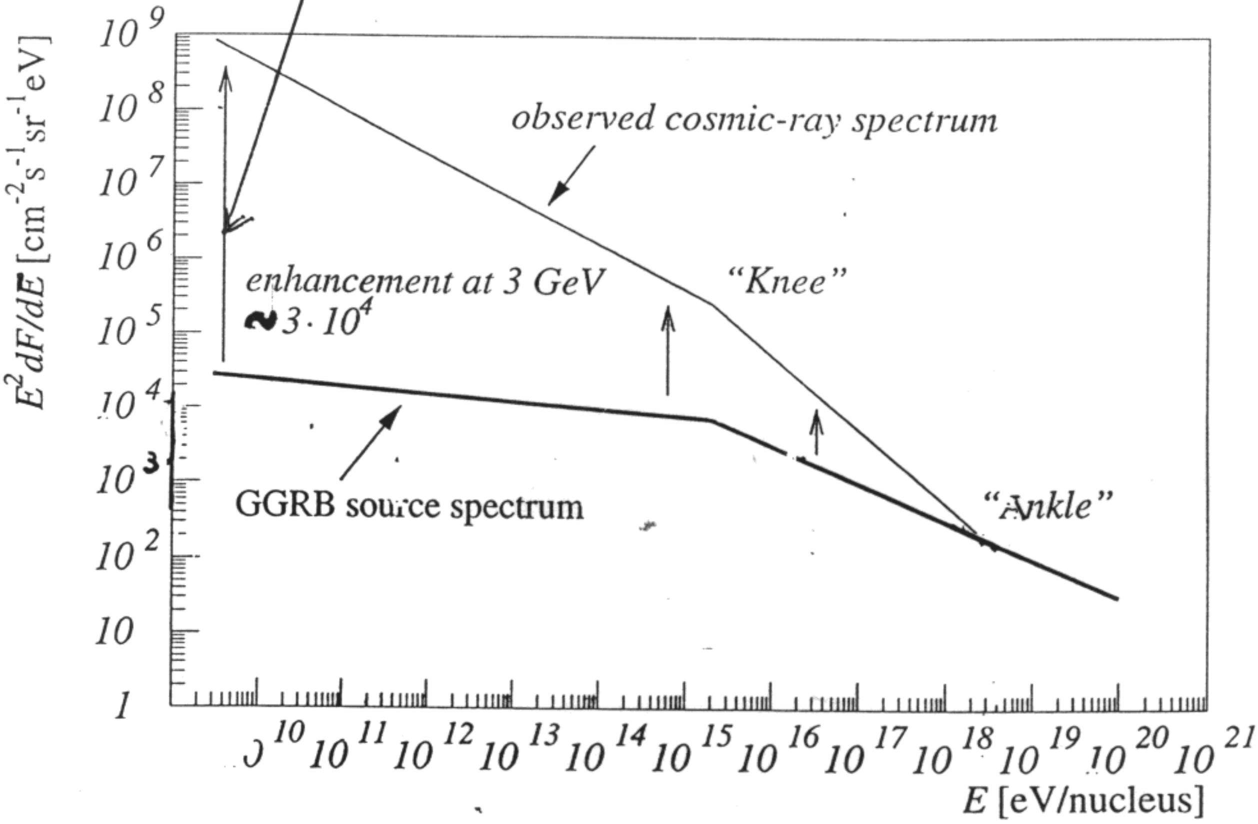

$$\frac{dn}{dE} \approx \tau(E)\left(\frac{dn}{dE}\right)_s \cong \begin{cases} C\,(E/E_{kn})^{-2.7} & E \le E_{kn} \\ C\,(E/E_{kn})^{-3.0} & E_{kn} \le E \le E_{an} \\ C\,(E_{an}/E_{kn})^{-3.0}(E/E_{an})^{-2.5} & E_{an} \le E < E_s \end{cases}$$

where

$E_{knee} \sim 2A\Gamma_3^2 \times 10^{15}$ eV

$E_{ankle} \sim 3\times 10^{18}(ZB_h/3\mu G)(\lambda/kpc)$ eV

$E_s \sim \Gamma A^2 Z^{-3/2}(R/c)^{-1/2} \times 10^{20}$ eV

THE HIGH ENERGY γ-RAY SKY IN GALACTIC COORDINATES SEEN BY EGRET/CGRO

30 MeV – 100 GeV

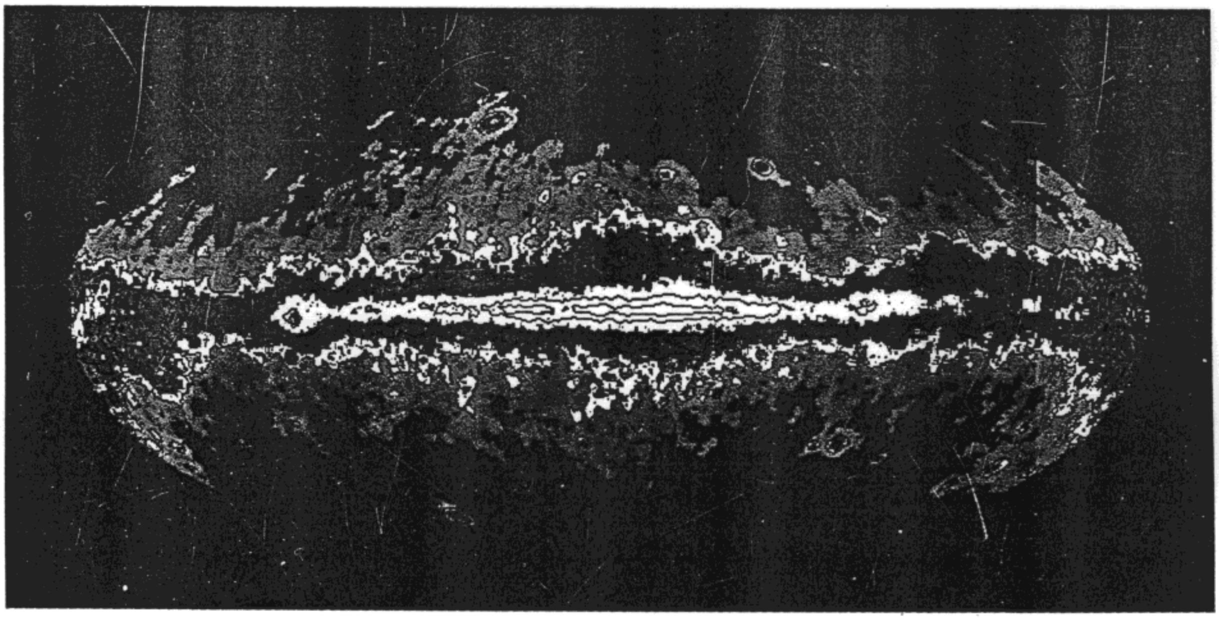

The Extragalactic Diffuse X-Ray and γ-Ray Background Radiations

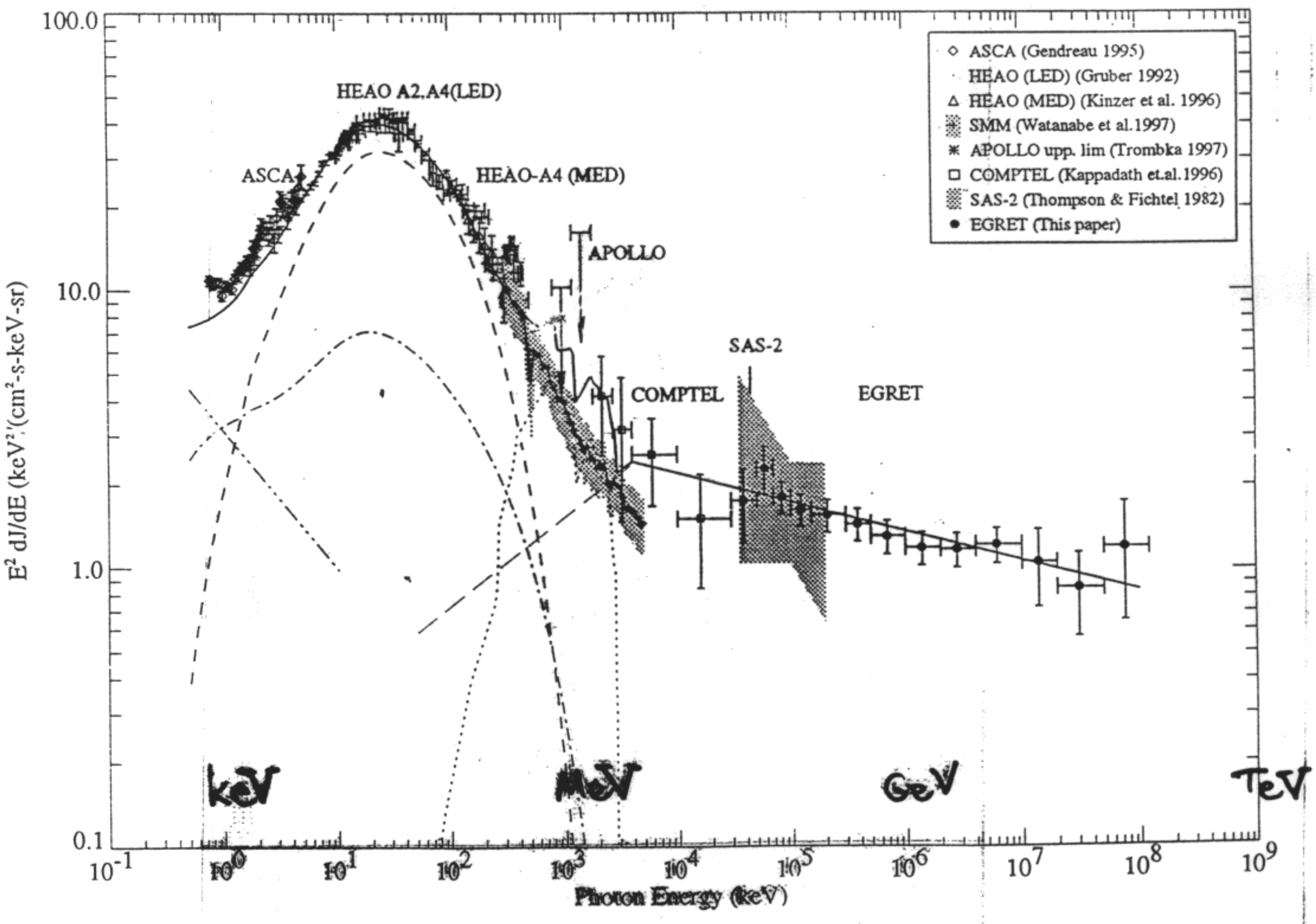

FIG. 10.—Multiwavelength spectrum of the extragalactic gamma-ray spectrum from X-rays to high-energy gamma rays. The estimated contribution from Seyfert I (*dot-dashed line*), and Seyfert II (*dashed*) are from the model of Zdziarski (1996); steep-spectrum quasar contribution (*triple-dot-dashed line*) is taken from Chen, Fabian, & Gendreau (1997); Type Ia supernovae (*dotted line*) is from The et al. (1993). The blazar contribution below 4 MeV (*long-dashed line*) is derived assuming the average blazar spectrum breaks around 4 MeV (McNaron-Brown et al. 1995) to a power law with an index of ~ -1.7. The thick solid line indicates the sum of all the components.

Cosmic Ray Electrons

Dar, De Rujula, Antoniou PRL (submitted)

$$\frac{dn_p}{dE} \sim E^{-2.7}$$

$$\Downarrow$$

$$\left(\frac{dn_p}{dE}\right)_s \sim \left(\frac{dn_e}{dE}\right)_s \sim E^{-2.2}$$

$$\Downarrow$$

Inverse Compton Cooling

$$\Downarrow$$

$$\boxed{\frac{dn_e}{dE} \sim E^{-3.2}}$$

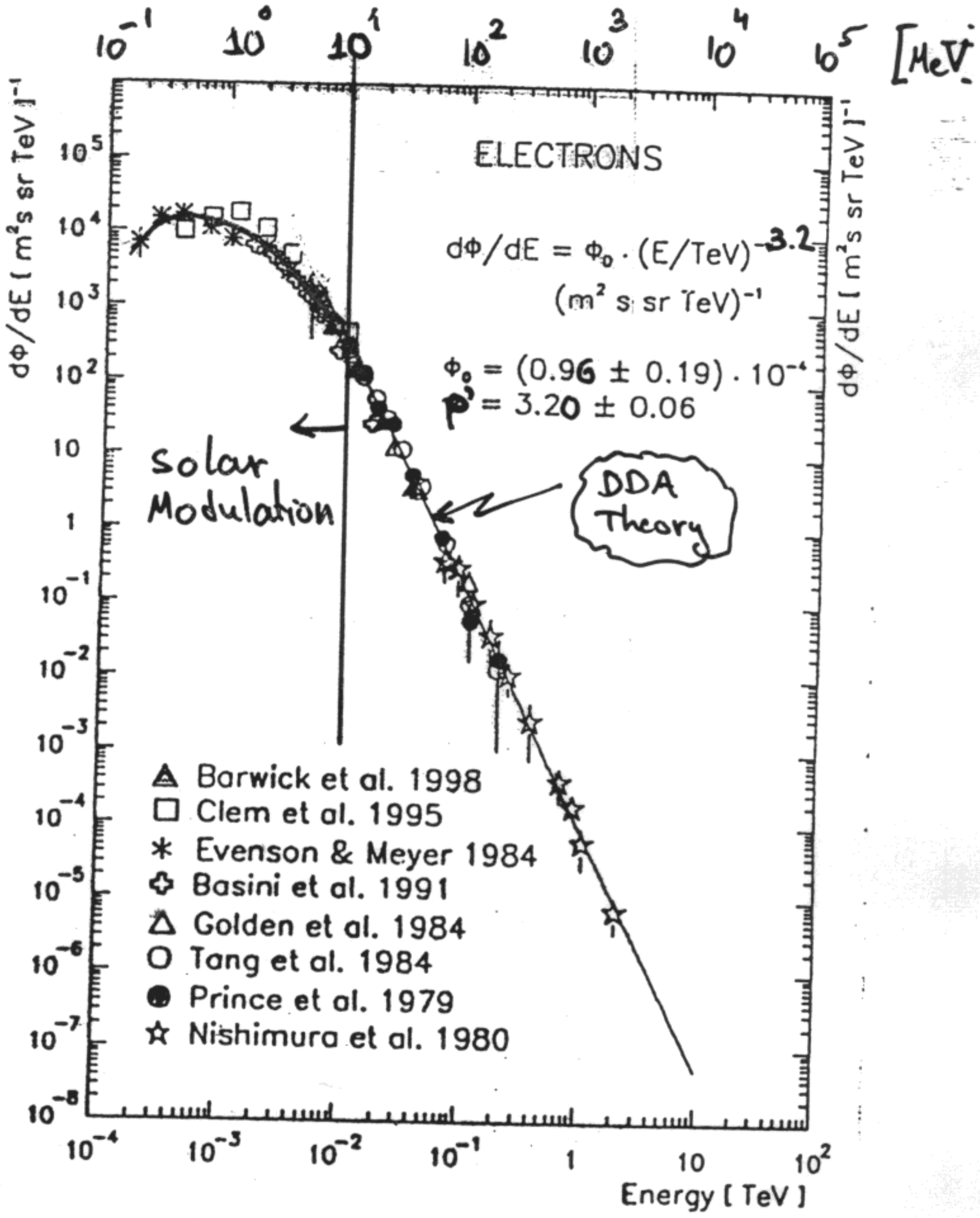

GBR:

$$e^- + \gamma \rightarrow e^{-\prime} + \gamma'$$

$$E_{\gamma'} \approx \frac{4}{3}\, \varepsilon_\gamma \left(\frac{E_e}{m_e c^2}\right)^2$$

MBR:

$\varepsilon_\gamma = 2.7\,kT \sim 6.36\times10^{-4}$ eV

$n = aT^3 = 411/\mathrm{cm}^3$

Production Rate Per Unit Volume:

$$\frac{dn_{\gamma'}}{dE} = \frac{dn_e}{dE_e}\, n_{BKG}\, \sigma_T\, c\, \frac{dE_e}{dE_{\gamma'}} \; ; \quad \sigma_T = 0.65\times10^{-24}\ \mathrm{cm}^2$$

if $\frac{dn_e}{\ldots} \sim E^{-p'} \Rightarrow \frac{dn_{\gamma'}}{\ldots} \sim E^{-\frac{p'+1}{2}}$; $\frac{p'+1}{2} = \frac{3.2+1}{2} = 2.1$

THE "EXTRAGALACTIC" DIFFUSE GAMMA RAY BACKGROUND RAD.

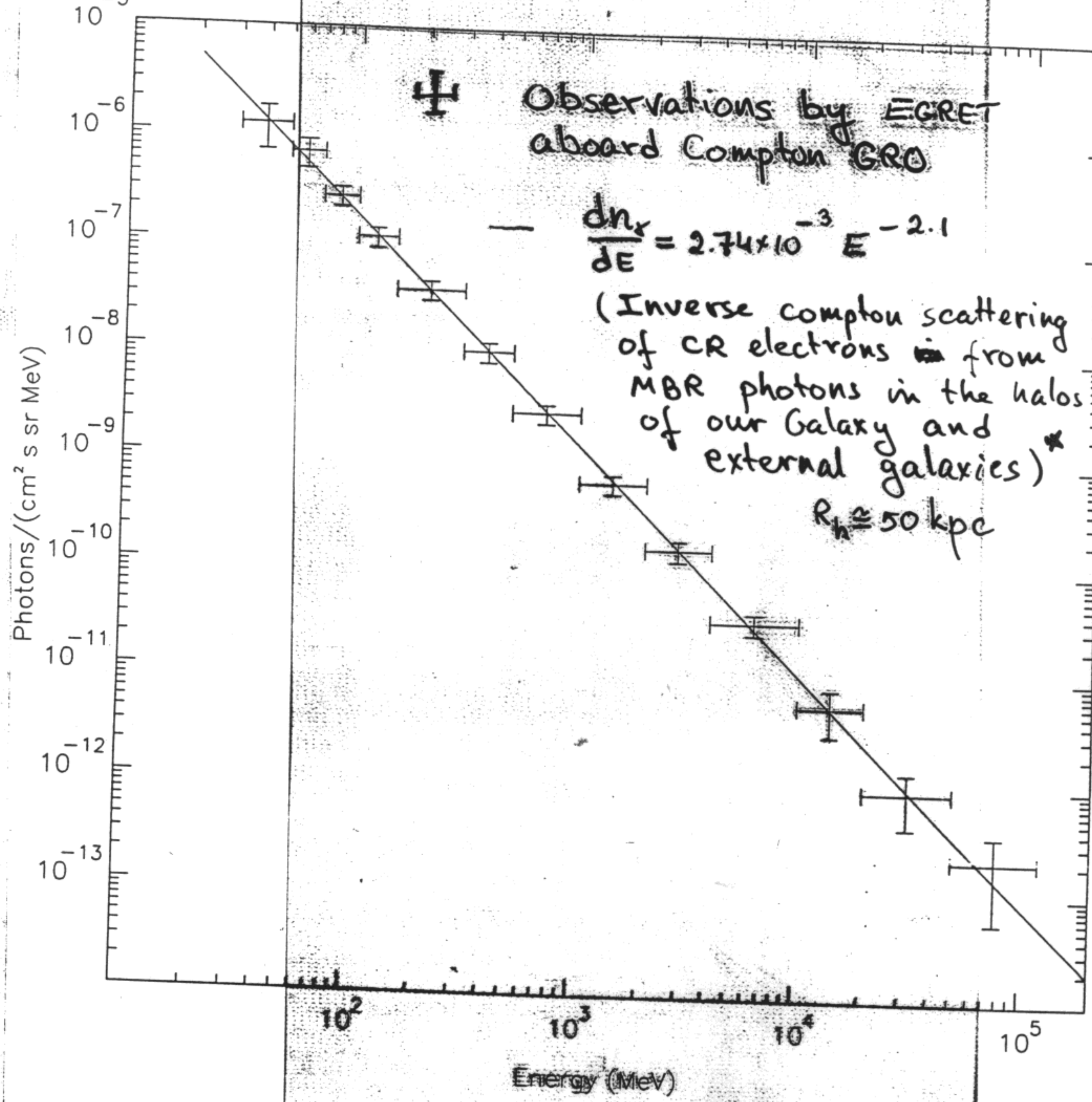

Dar, DeRujula, Antoniou, Submitted to PRL
(astro-ph/9901004)

$$\frac{dF_\gamma}{dE} = \frac{dF_\gamma^{MW}}{dE}\left[1 + \frac{4\pi R_h^2}{3}\,\frac{\rho_L}{L_*}\,\frac{c}{H_0}\int_1 \frac{R_{SFR}(y)}{R_{SFR}(0)}\,\frac{y}{f(y)}\,\frac{dy}{y^3}\right]$$

THE RADIO HALO OF THE EDGE-ON GALAXY

NGC 5775

$\theta_i \approx 84^\circ$

$d \approx 28.6$ Mpc

$$\frac{dN_e}{dE} \simeq E^{-\beta}$$

$\beta_{disk} \sim 2.2$

$\beta_{halo} \sim 3.2$

$43 \times 22 \; (\mathrm{kpc})^2$

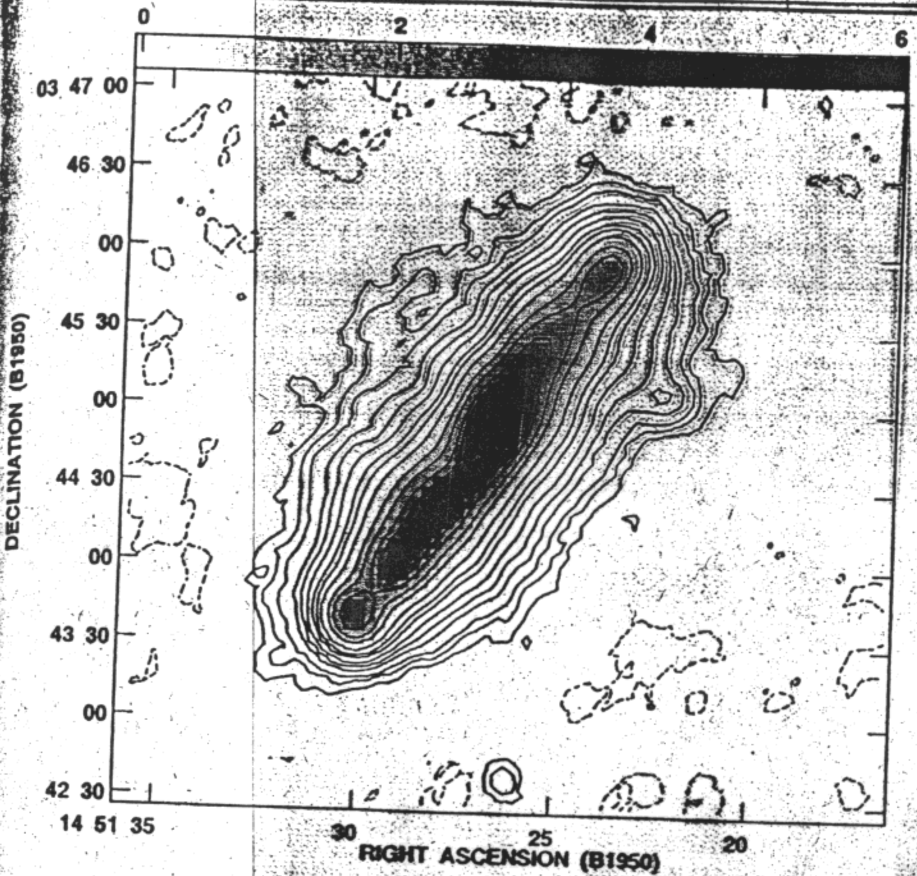

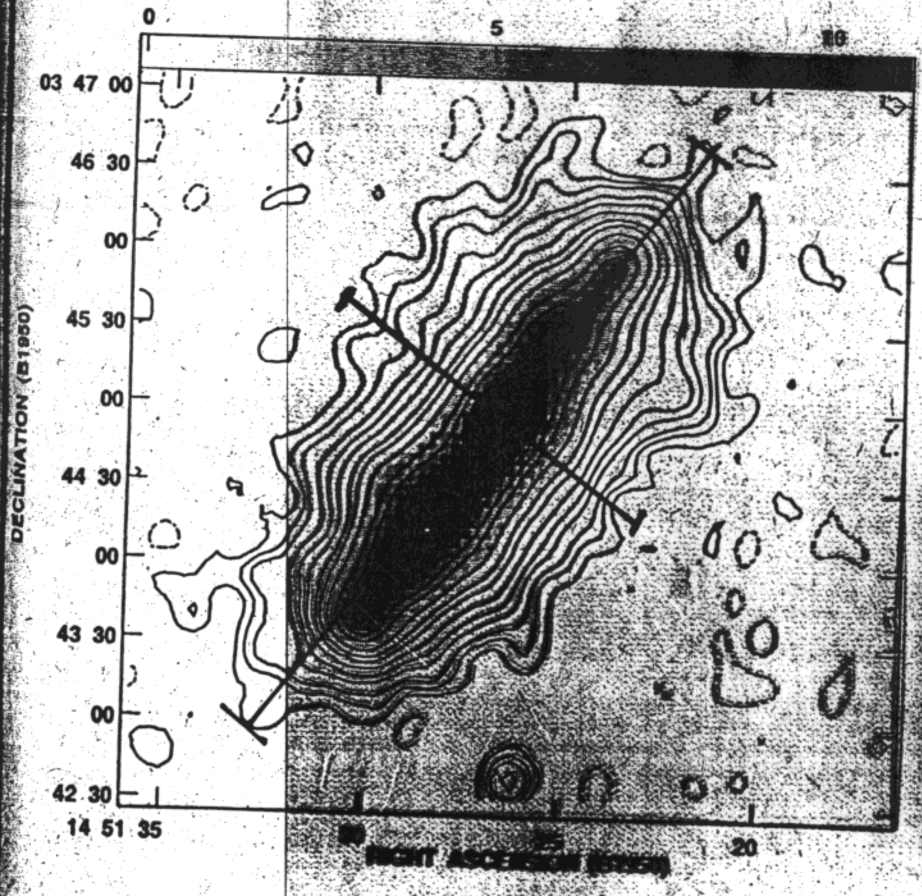

Fig. 2. a The 20 cm radio continuum image used in the analysis. With a restoring beam of 15″ × 13″, it represents the net result of combining the B, C and D array data. The *rms* noise in this map is 25 μJy/beam. The contours represent 1, 2, 3, 5, 7, 10, 15, 20, 30, 50, 70, 100, 125, 150, 175, 200, 300, 500, 750 and 1000 times 70 μJy/beam. b The 6 cm continuum image used in the analysis. With a restoring beam of 15″ × 13″, it represents the result of combining the C and D array data. The rms noise in this map is 25 μJy/beam. The contours represent 1, 2, 3, 5, 7, 10, 15, 20, 30, 50, 70, 100, 125, 150, 175 and 200 times 30 μJy/beam.

Duric et al. A&A

Conclusions

- Highly relativistic jets (plasmoids) ejected in the birth, death or collapse of NS may produce the

  1. GRBs
  2. Cosmic Rays

- GRB are highly collimated

  $\Delta\Omega \sim \pi/\Gamma^2 \sim 10^{-6}$; $E_k \sim 10^{52}$ erg ; $E_\gamma = \eta E_k$

  $\eta \sim 10^{-6}$

- The "true" rate of GRB

$$R_{GRB} \sim 10^3 \times \frac{4\pi}{\Delta\Omega} y^{-1} \sim 10^{10} y^{-1}$$

Observed

- The "true" rate per Milky Way like Galaxy

$$\frac{R_{GRB}}{\text{"}N_G\text{"}} \sim 2\times10^{-2}\left(\frac{N_G}{10^{11}}\right)^{-1}\left(\frac{\Gamma}{10^3}\right)^2 y^{-1} \sim R_{NS}$$

  similar to the NS Birth Rate

- Galactic "GRBs" produce the observed CR

- The GRB remnants are:

  1. Soft Gamma Ray Repeaters

     Precessing Jets From Cooling/Spinning Down NS

  2. Hot Spots (Mini Lobes) in the Galactic Halo

- The jets transport the "GRB" energy into the Galactic hab producing there the

Do GRBs Have a Second Bump ?
Like, e.g.,

Mrk 421 / Multiwavelength Spectrum

$z = 0.031$

$D \sim \frac{zc}{H_0} \approx 140\ \text{Mpc}$

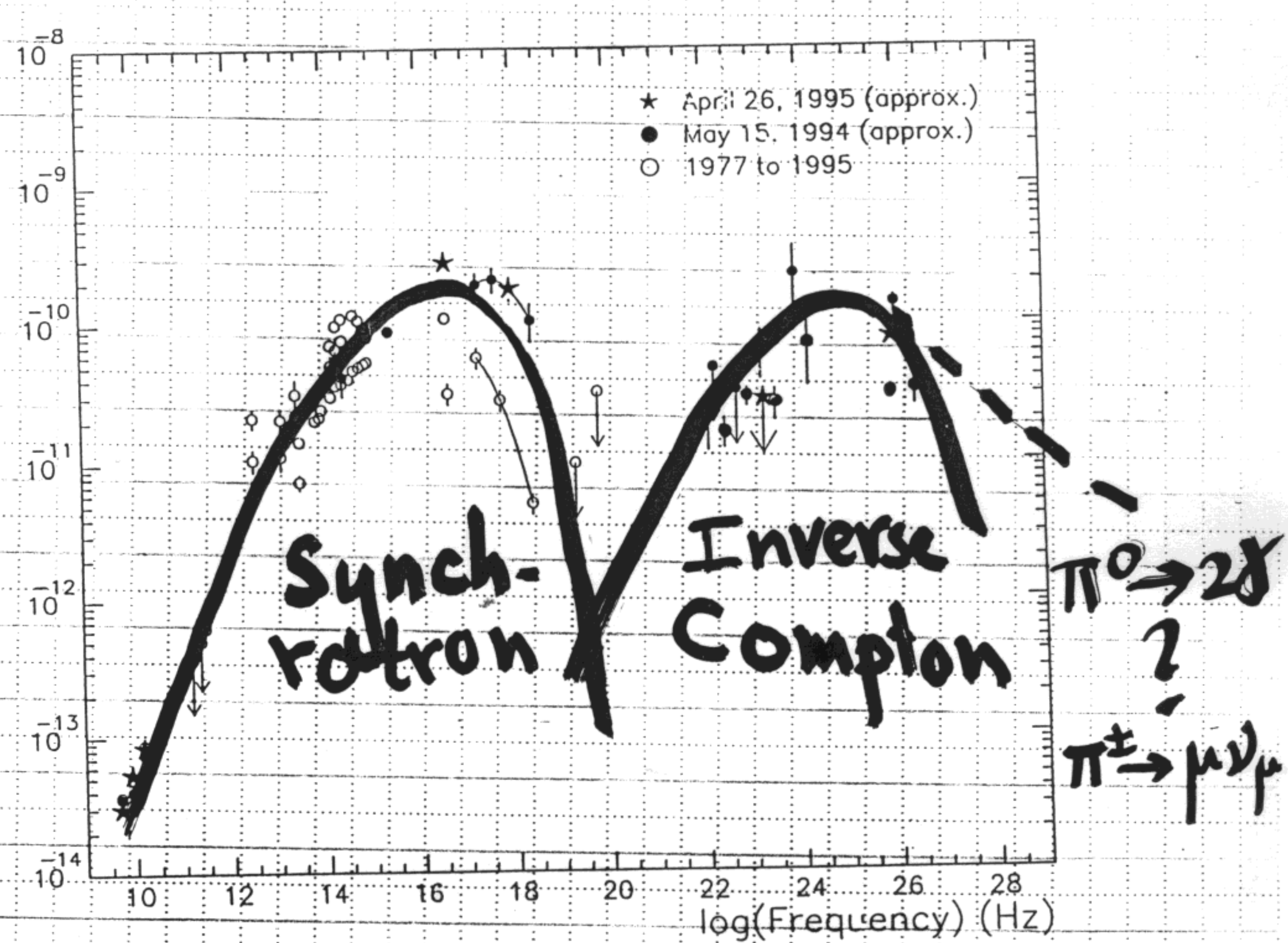

Why Mrk 501 was not detected by EGRET ?

Why BL LAC 0521-365 2200+420 1219+285

$z =$ 0.055 0.069 0.102

$N > 10^{22}\,cm^{-2}$; Evidence For "Target" Material

$$F_\nu = F_0\,\nu^a t^b e^{-\tau(\nu,z)} \qquad a = 2b/3 = \frac{p-1}{2}$$

Extinction In The Source ?